TWO-DIMENSIONAL GEOELECTRICAL RESISTIVITY IMAGING OF THE AHMADU BELLO UNIVERSITY TEACHING HOSPITAL (ABUTH) PREMISES, SHIKA, ZARIA, NIGERIA.

BY

INICHINBIA SONNY
B.Sc. PHYSICS (PHC 2000)
MSC/ SCI/ 44893/ 2004-05

BEING A RESEARCH THESIS SUBMITTED TO THE POSTGRADUATE SCHOOL, AHMADU BELLO UNIVERSITY, ZARIA, NIGERIA

IN PARTIAL FULFILMENT OF THE REQUIREMENTS FOR THE AWARD OF MASTER'S DEGREE (M. Sc.) IN APPLIED GEOPHYSICS.

DEPARTMENT OF PHYSICS
FACULTY OF SCIENCE
AHMADU BELLO UNIVERSITY, ZARIA,
NIGERIA.

DECEMBER, 2007

DECLARATION

I hereby declare that:

The research work presented in this thesis entitled "**TWO-DIMENSIONAL GEOELECTRICAL RESISTIVITY IMAGING OF THE AHMADU BELLO TEACHING HOSPITAL (ABUTH) PREMISES, SHIKA, ZARIA, NIGERIA**", has been performed by me in the Department of Physics under the supervision of **Prof. I. B. Osazuwa (FNIP)** and **Dr. P.O. Sule**.

The information derived from the literature has been duly acknowledged in the text and a list of references provided. No part of this research thesis was previously presented for another degree or diploma at any university.

INICHINBIA, Sonny
MSC/SCI/44893/2004-05 ---------- ----------
--

Signature **Date**

CERTIFICATION

This research thesis entitled "**TWO-DIMENSIONAL GEOELECTRICAL RESISTIVITY IMAGING OF THE AHMADU BELLO UNIVERSITY TEACHING HOSPITAL (ABUTH) PREMISES, SHIKA, ZARIA, NIGERIA**", by **INICHINBIA**, **Sonny** meets the regulations governing the award of degree of Master of Science (M.Sc.) of Ahmadu Bello University, Zaria, and is approved for its contributions to knowledge and literary presentation.

---------- **Date**----------

Prof. I. B. Osazuwa
Chairman, Supervisory committee

---------- **Date**----------

Dr. P. O. Sule
Member, Supervisory committee

---------- **Date**----------

Prof. N. Hariharan
Head, Department of Physics

---------- **Date**----------

Prof. S. A. Nkom
Dean, Postgraduate School

DEDICATION

This research thesis is dedicated to the Almighty God for His guidance, provision and all His goodness throughout the programme. This research thesis is also dedicated to all geophysicists because of its contributions to this dynamic field of study and research.

ACKNOWLEDGEMENT

First and foremost, I express my sincere thanks and appreciation to God Almighty for His countless blessings upon me and for enabling me to achieve this important milestone in my life.

Thanks to my supervisors, Prof. I. B. Osazuwa (FNIP) and Dr. P. O. Sule. I appreciate your efforts for finding time to go through this work despite your busy schedule.

I also want to in a special way thank Prof. I. B. Osazuwa through whom financial grants and equipment donated by the International Program in the Physical Sciences (IPPS), Uppsala University Sweden was made available to me. This greatly enhanced the completion of this work. Sir, I appreciate you and the almighty God bless you.

To my parents, Mr. and Mrs. Inichinbia Frank, and my most elderly brother, Mr. Miabiye Ebenezer Kalio and the entire members of the family, I say thanks to you all for your prayers and support. I am greatly indebted to you all.

I am also grateful to Wg. Cdr. Abdullahi A. Kassimu, Akaolisa Casmir C. Zanders, Gabriel N. Egwuonwu, Stephen O. Ibe, Chinedu Ani, Adetola Oniku and Mallam Nasiru Khalid Abdullahi for their immense contributions to the success of this work. God bless you sirs.

Finally, my sincere gratitude goes to Mr. Ibifuro Banigo, Chiemeke, Collins C., Bro. Godwin John, Bro. Gideon A. Bobai, and Bro. Moses Unogwu Ogaba, Bro. Bello

Bisalla, Bro. James Ohambele, Bro. Dele Abogunrim and to all my friends, colleagues and well-wishers for their invaluable contributions to enable me succeed in this programme.

Special thanks to Joseph Orojah Osumeje and Omobolaji Teslim Lawal who painstakingly edited the entire work. Thanks my brothers and God bless you. Many thanks to Mummy too.

My special thanks and appreciation go to both the leadership and members of the Deeper Life Campus Fellowship (DLCF), Ahmadu Bello University, Zaria, for their physical and spiritual support towards me, which has preserved and sustained me in the faith until now. God bless you all in Jesus name. Amen.

That a name is not mentioned here is not meant to disregard many others that contributed in whatever form, but the omission is as a result of space constraint. Please pardon me and thank you all.

ABSTRACT

The Ahmadu Bello University Teaching Hospital (ABUTH) is located along Zaria-Funtua road, Shika, which is situated on the crystalline metamorphic rocks of the northern Nigerian Basement Complex. It lies between latitudes 11^{o} $7^{/}$ N and 11^{o} $24^{/}$ N and longitudes 7^{o} $31^{/}$ E and 7^{o} $50^{/}$ E and has an elevation of about 650 m – 700 m above mean sea level.

The aim of this survey is to carry out a Two-Dimensional Geolectrical Resistivity Imaging of the subsurface in the area. The objectives of the survey were to determine the thickness of the overburden and the weathered basement, to resolve the overburden layering and to evaluate the groundwater potential of the area; thus characterizing the geologic setting at the surveyed area.

A modern and state-of-the-art field instrument, the ABEM Automatic LUND Imaging System (Terrameter SAS 4000 and ES 464), produced by ABEM instrument AB, was used to accomplish this task. This uses multi-core cables with takeouts at 5 m intervals, having a total of 42 electrodes covering a spread of 200 m.

Six profiles were covered and the data was processed to display the variations of electrical resistivities using the RES2DINV software. The results of this survey in correlation with borehole data revealed three distinct layers: the overburden which is about 16 m - 26 m thick having a resistivity range of about 194 Ωm – 1759 Ωm. The weathered basement which is appreciably thick (about 5 m – 14 m), is highly fractured and weathered, so constitutes a good aquifer having a resistivity range of about 0.687 Ωm – 678 Ωm. and the fresh crystalline basement having a resistivity of about 1223 Ωm. The fresh crystalline rock is at a variable depth of about 21 m - 40 m below the surface.

TABLE OF CONTENTS

TITLE PAGE i

DECLARATION ii

CERTIFICATION iii

DEDICATION iv

ACKNOWLEDGEMENT v

ABSTRACT vii

TABLE OF CONTENTS viii

LIST OF TABLES xi

LIST OF FIGURES xii

CHAPTER ONE

INTRODUCTION

1

1.1 GENERAL OVERVIEW 1

1.2 THE SURVEY AREA 5

1.3 LOCATION AND ACCESSIBILITY OF THE STUDY AREA 7

1.4 CLIMATE AND VEGETATION 9

1.5 GENERAL GEOLOGY OF THE STUDY AREA IN ZARIA SHEET 102 9

1.6 HYDROGEOLOGY 15

1.7 PREVIOUS GEOPHYSICAL SURVEY OF THE AREA AND ITS ENVIRON 17

1.8 AIM AND OBJECTIVES OF THE SURVEY 18

1.6 SCOPE AND LIMITATIONS OF THE SURVEY 19

CHAPTER TWO

PRINCIPLES AND INSTRUMENTATION 21

2.1 IMPORTANCE AND USES OF ELECTRICAL IMAGING 22

2.2 THEORY 23

2.3 WENNER ARRAY 29

2.4 THE CONCEPT OF APPARENT RESISTIVITY 30

2.5 TYPICAL RESISTIVITY VALUES OF EARTH MATERIALS 31

2.6 INSTRUMENTATION 35

2.7 THE ABEM LUND IMAGING SYSEM 35

CHAPTER THREE

METHODOLOGY 39

3.1 CHOICE OF THE METHOD 39

3.2 RECONNAISSANCE SURVEY 40

3.3 FIELD PROCEDURE 40

3.4 PSEUDOSECTION PLOTTING 43

CHAPTER FOUR

FIELD RESULTS AND INTERPRETATION 46

4.1 DATA PROCESSING 47

4.2 INTERPRETATION TECHNIQUE 50

4.3 GEOLOGICAL CONTROL 52

4.4 FIELD RESULTS 52

4.5 GEOLOGIC SECTION FROM BOREHOLE DATA 66

4.6 RESISTIVITY VALUES FROM RESEARCH WORK 73

4.7 TYPICAL RESISTIVITY VALUES FROM PREVIOUS WORKS 73

CHAPTER FIVE

DISCUSSION OF RESULTS, SUGGESTIONS AND CONCLUSIONS 76

5.1. DISCUSSION ON RESULTS 76

5.2 GROUNDWATER POTENTIALS 77

5.3 SUGGESTIONS FOR FURTHER WORK 78

5.4 CONCLUSIONS 79

REFERENCES 80

LIST OF TABLES

2.1 APPLICABILITY OF THE DIFFERENT RESISTIVITY AND INDUCED POLARIZATION METHODS 22

2.2 ELECTRICAL RESISTIVITY OF SOME KIND OF NATURAL WATERS 34

4.1 RESISTIVITY VALUES FROM THE RESEARCH WORK 73

4.2 a & b TYPICAL RESISTIVITY VALUES COMPILED FROM PREVIOUS WORKS 74

LIST OF FIGURES

1.1 MAP OF THE SURVEY AREA 6

1.2 LAYOUT OF EXPERIMENTAL PROFILES IN THE SURVEY AREA 8

1.3 GEOLOGICAL MAP OF SHIKA SHEET 102 14

2.1 CURRENT AND POTENTIAL DISTRIBUTION WITHIN HOMOGENEOUS AND ISOTROPIC EARTH 25

2.2 WENNER ALPHA, BETA AND GAMMA ARRAYS SHOWING DIFFERENT ELECTRODE POSITIONS 30

2.5 A TYPICAL RANGE OF RESISTIVITIES OF GEOLOGIC MATERIALS 33

2.6 ABEM LUND IMAGING SYSTEM TOGETHER WITH SAS 4000 USED FOR ELECTRICAL RESISTIVITY TOMOGRAPHY 38

3.1 TYPICAL ELECTRODE LAYOUT OF WEN32SX: WENNER CVES WITH TWO CABLES USING THE TERRAMETER SAS4000 AND ES464 IN LUND IMAGING 43

3.2 PRINCIPLE FOR BUILDING UP A PSEUDOSECTION 45

4.1 ARRANGEMENT OF THE BLOCKS USED IN A MODEL TOGETHER WITH THE DATUM POINTS IN THE PSEUDOSECTION 50

4.2 THE RESULT OF 2D INVERSION OF THE WENNER-ARRAY DATA ALONG SURVEY LINE 1, IN ABUTH HOSTELS 55

4.3 THE RESULT OF 2D INVERSION OF THE WENNER-ARRAY DATA ALONG SURVEY LINE 2, IN ABUTH HOSTELS 57

4.4 THE RESULT OF 2D INVERSION OF THE WENNER-ARRAY DATA ALONG SURVEY LINE 3, IN ABUTH HOSTELS 59

4.5 THE RESULT OF 2D INVERSION OF THE WENNER-ARRAY DATA ALONG SURVEY LINE 4, IN ABUTH RESIDENTIAL QUARTERS 61

4.6 THE RESULT OF 2D INVERSION OF THE WENNER-ARRAY DATA ALONG SURVEY LINE 5, IN ABUTH RESIDENTIAL QUARTERS 63

4.7 THE RESULT OF 2D INVERSION OF THE WENNER-ARRAY DATA ALONG SURVEY LINE 6, IN ABUTH RESIDENTIAL QUARTERS 65

4.8 GEOLOGICAL WELL-LOG OBTAINED BY PREUSSAG LTD 68

4.9 GEOLOGICAL WELL-LOG OF SHIKA OBTAINED FROM THE NWRI 2, MANDO, KADUNA STATE 70

4.10 GEOLOGICAL WELL-LOG OF ABUTH HOSTELS OBTAINED FROM THE NWRI 1, MANDO, KADUNA STATE 72

CHAPTER ONE

INTRODUCTION

1.1 General Overview

Geophysical investigations of the earth involve studying the physical properties of the earth to provide vital information on subsurface material conditions for numerous practical applications. These are done by taking measurements at or near the earth's surface that are influenced by the internal distribution of physical properties. Consequently, analysis of these measurements can reveal how the physical properties of the earth's interior vary vertically and laterally that reflect the subsurface geology. Another method of investigating subsurface geology is of course by drilling and pitting which provide information only at discrete locations and are expensive.

Geophysical investigations are non-intrusive and non-invasive, thus avoiding the disruption caused by intrusive investigations such as drilling and pitting. Geophysical investigations cover large site areas rapidly and optimize the targeting of necessary intrusive inspections. In environments where intrusive investigations are not permissible, geophysics is the only answer. The methods employed include gravity, magnetics, seismic, resistivity, induced polarization, self potential, radiometrics, ground penetrating radar, electromagnetic methods, etc. These methods are cost effective and capable of detecting and delineating local features of interest. For instance for groundwater exploration, electrical resistivity and seismic methods are most appropriate while gravity is a subsidiary method to the two (Keary and Brooks, 1988).

Pressure on natural resources from growing populations, with increasing demand for water supply, infrastructure and housing, has increased over the past decades and can be expected to rise continually. Further, stress on the environment due to pollution will increase the need for detailed geological knowledge, for geotechnical,

hydrogeological and environmental protection purposes. Geophysical methods can play an important role in the acquisition of such knowledge. However, the complete survey procedure, including data acquisition, data processing, interpretation and presentation must be efficient in terms of time, cost and manpower. It is also essential to ensure a continuous cover, along transects or over an area to complement point information obtained from traditional methods such as drilling, test pits, mechanical sounding, etc. This implies that at least two-dimensional (2D) information is required, and a number of 2D sections may be combined to build a 3D picture (Dahlin, 1996).

One of the new developments in recent years is the use of 2D electrical imaging/tomography survey to map areas with moderately complex geology (Griffiths and Barker, 1993). Such surveys are usually carried out using a large number of electrodes, 25 or more, connected to a multi-core cable. Resistivity surveys measure variation in the electrical resistivity of the ground by applying small electric current across arrays of ground electrodes. Electrical resistivity is a function of porosity, fluid saturation, resistivity of the pore fluid and the solid, and the material texture among others. Resistivity imaging is particularly useful in clayey ground where methods such as the ground penetrating radar GPR are less effective and helps define translational boundaries that are difficult to detect using other geophysical methods.

Using a version of the Microprocessor-controlled Resistivity Traversing (MRT) System, employing the Campus GEOPULSE meter, revealed that in areas of modest subsurface geological complexity where some control is available and where the structures are essentially two-dimensional, then good approximations to the true geoelectrical sections can be obtained down to depths of between 100m and 200m (Griffiths *et al.*, 1990).

Using the Microprocessor-controlled Resistivity Traversing (MRT) System, boreholes have been sited in the crystalline basement areas of Nigeria (Olayinka and Barker., 1990).

Electrical resistivity imaging has been used for 'imaging fractures in hardrock terrain'. This has revealed that where fractures are present, the bedrock is expected to be more strongly weathered to a greater depth than where it is not fractured. For this reason it is best to drill at points where the bedrock reaches its greatest depth for thick reservoir of water in the overburden and the likelihood of the reservoir being underlain by bedrock that is fractured (Barker, 2001).

Electrical Resistivity Imaging (ERI) technique had been applied for borehole siting in hardrock (granitic and gneissic basement) regions of India, (Barker *et al*., 2001). Using the Wenner array with a manual imaging system connected to an SSR MPL resistance meter manufactured in India, by IGIS Ltd, Hyderabad, this new electrical tomography (imaging) technique provided detailed 'pictures' of the subsurface that showed variation in bedrock topography and the nature and thickness of the overburden. The resulting images were used to plan borehole investigations more cost effectively.

The Electrical Resistivity Imaging technique was applied to develop a geological model for a proposed Edmonton landfill site. The Sting/Swift^{TM} (Advanced Geosciences Inc., Austin, Tex.) ERI System was used to further resolve and characterize the geologic setting at the proposed Aurum solid-waste landfill site near Edmonton, Alberta (Meads *et al*., 2003).

Resistivity tomography using a Wenner configuration was carried out as an aid to planning gas-pipeline construction, in Risha area, north-east Jordan. A 2D ERT measurement was conducted using the Iris Sycal R2 resistivity instrument to map the

ground resistivity in advance of gas-pipeline construction in the Risha area, north-east Jordan. It also served to detect areas of high ground conductivity due to clays or saline soils, which can create conditions in which pipeline corrosion is, accelerated. This case study revealed that electrical resistivity tomography (ERT) can be used effectively for infrastructure planning (Batayneh, 2006).

A '2D data modelling by electrical resistivity tomography for complex subsurface geology', has been constructed. This is a new tool for 2D apparent-resistivity data modelling and inversion with the purpose of handling the inversion results. For instance, this was found to be effective to correct reconstructed models and to check the effects of such changes on the calculated apparent resistivity. Tests on synthetic and real data, in particular in handling indeterminate cases, showed that the flexible approach is a good way to build a detailed picture of the proposed area (Cardarelli and Fischanger, 2006). Also a two-dimensional inversion of vertical sounding data revealed the deep resistivity structure of the Dikili-Bergama region, west Anatolia, showing very low resistivity near the Dikili and Kaynarca hot springs. The 2D inversion results also indicated the presence of fault zones striking nearly N-S and E-W, and fault bounded graben-horst structures that show promising potentials for geothermal field resources (Özürlan, *et al*., 2006).

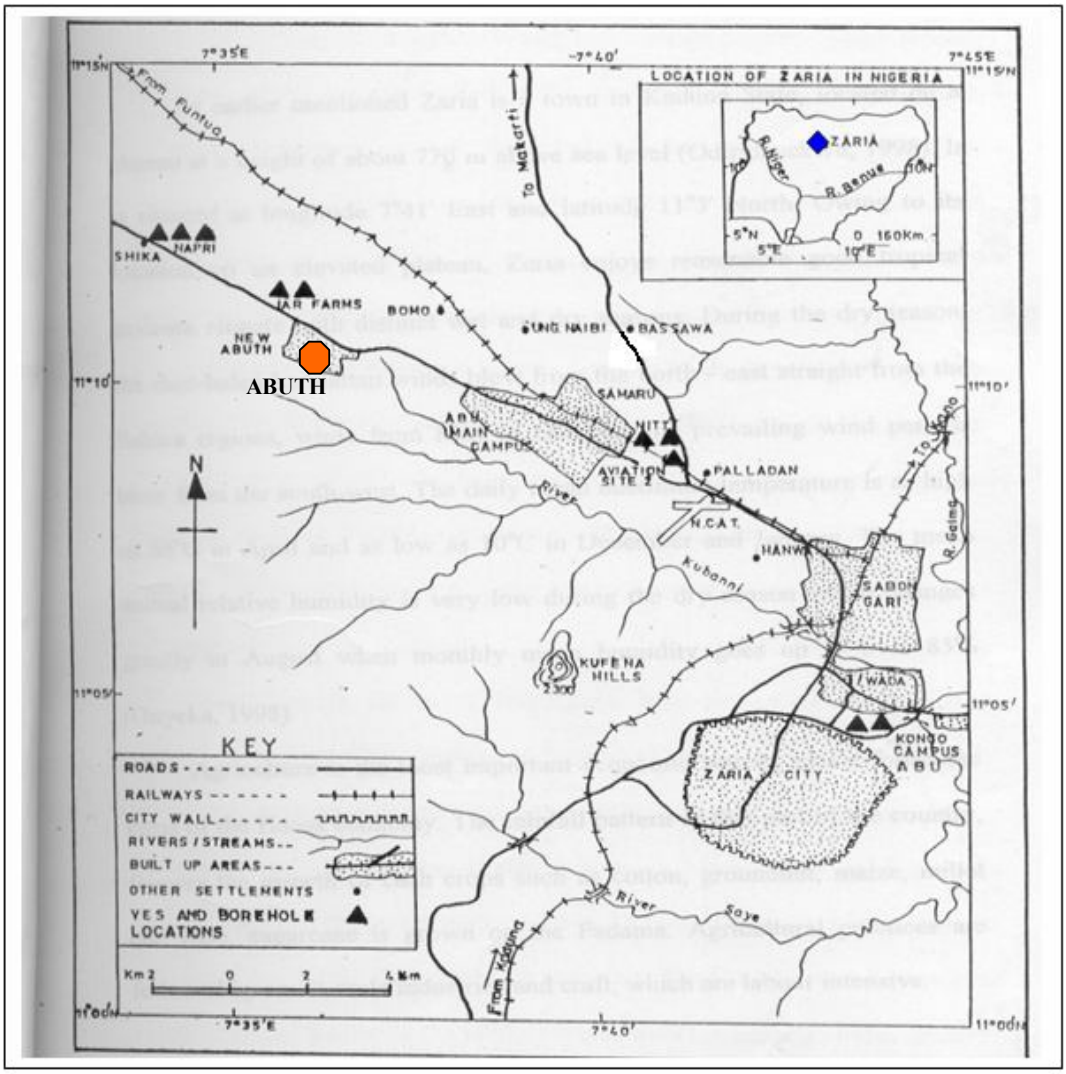
Electrical resistivity survey is a non-destructive and cost effective method and has the advantage of rapid data collection and interpretation. Two or three people could conveniently achieve 5 – 7 long electrical profiling lines each day, at a normal production rate. Thus, the use of multi-electrode systems for the data acquisition allows a dramatic increase in field productivity. Since ultimately the test of a new technique is its success in the field, the method adopted for this research thesis was the 2D Geolectrical Resistivity Tomography using the ABEM LUND Imaging System. The

ABEM LUND Imaging System is a multi-electrode system for cost effective and high-resolution 2D and 3D resistivity surveys. The included data acquisition software supports 2D and 3D surveys with surface arrays which may also be used for borehole measurements. The data can be inverted automatically to provide an image of true resistivity. It is the automatic nature of this process of interpretation which enables it to be termed "imaging''. No apriori information on the distribution of resistivity is involved and the resulting image is free from interpreter bias (Griffiths and Barker, 1993).

A Wenner array with *protocol*, WEN32SX was carried out to map the electrical properties as an aid to characterizing the ground conditions. In the present survey, a 5m interval between 41 electrodes was employed with each spread having a length of 200m. The survey data was processed to produce graphic depth sections of the thickness and resistivity of the subsurface electrical layers. The resistivity sections are correlated with ground interfaces such as soils and fill layers or soil-bedrock interfaces to provide engineers with detailed information on subsurface ground conditions. However, the results of analyzing the 2D Wenner resistivity sections based on 2D inversion of field data and borehole information are presented.

1.2 The Survey Area

Shika is situated within the northern Nigerian Basement complex, (figure 1.1). It lies between latitudes $11^{o}\ 70^{/}$ N and $11^{o}\ 24^{/}$ N and longitudes $07^{o}\ 31^{/}$ E and $07^{o}\ 50^{/}$ E within the Zaria sheet 102. The mean elevation of the area is about 650 m – 700 m above mean sea level.



Survey Area ABUTH
Zaria

Figure 1.1 Location Map of the Survey Area from Geology Department, A.B.U. Zaria.

1.3 Location And Accessibility Of The Study Area

The Ahmadu Bello University Teaching Hospital (ABUTH) is located in Shika, along Zaria-Funtua road north of Ahmadu Bello University main campus. It lies between latitudes 11.18^{o} N and 11.17^{o} N and longitudes 07.60^{o} E and 07.61^{o} E. It is bordered by Zaria Academy in the north, Bomo village in the northeast, Area C A.B.U. staff quarters, Institute for Agricultural Research (IAR) farm and its dam.

Accessibility of the ABUTH is only by the Zaria-Funtua road which is a prominent federal road. All season motorable roads, some of which are tarred exist within the premises. Figure 1.2 is a sketch of the Ahmadu Bello University Teaching Hospital (ABUTH), showing the investigated site.

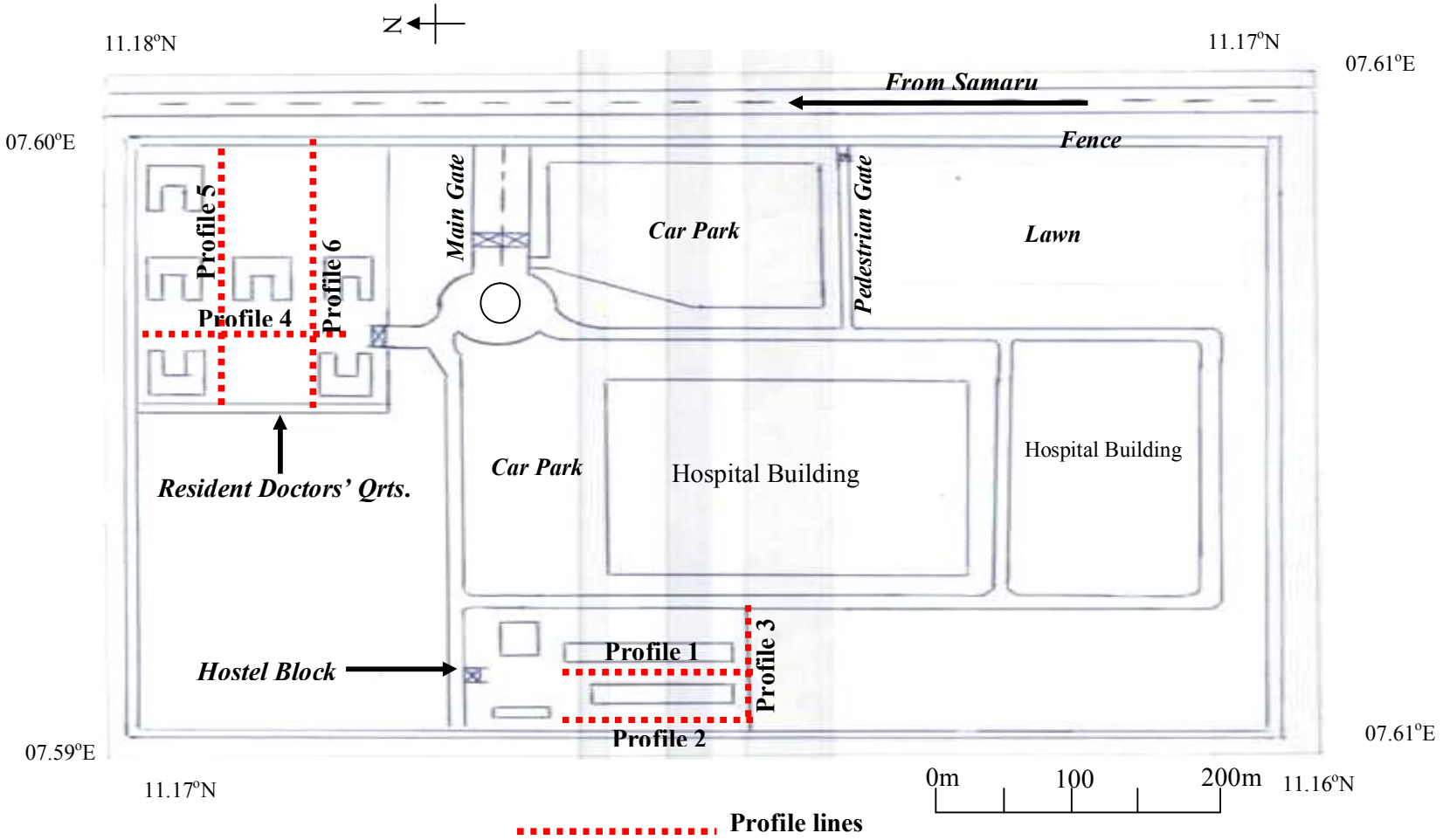


Figure 1.2 Layout of Experimental Profiles in the Survey Area

1.4 Climates and Vegetation

The area is in the Guinea Savannah climatic belt of Nigeria with distinct dry and wet seasons. The land surface is covered by vegetation which is typical to the Savannah grassland characterized by shrub bushes generally less than 3 m high and interrupted by large isolated trees. Normally a thick vegetation cover helps to trap rainwater and prevent severe surface run-off which usually gives rise to high erosion and gullying. Though the vegetation is scanty, thus, permitting erosion it is still of advantage in arresting the depletion of groundwater and reducing the rate of evapotranspiration.

1.5 General Geology of the Study Area in Zaria Sheet 102

Nigeria lies in the Pan-African mobile belt, which has been affected by Pan-African events through the ages of orogenic, epeirogenetic, tectonic and metamorphic cycles. The geology of Nigeria is classified into two parts, the Basement complex and the Sedimentary basins. The Ahmadu Bello University Teaching Hospital permanent site, Shika, lies on a plain which forms part of the vast gentle undulating plain scenery which extends almost unbroken from Sokoto and from the south of Kaduna (Joda, 1990). The soil is ferruginous with clay (Kaolinite) and some weathered minerals present.

The study area falls under the Nigerian Basement complex underlain by Precambrian rocks, so the geology of the area is the same as that of the Nigerian Basement complex. The rocks of the Basement complex occupy more than 50% of the total land surface of Nigeria, and accommodate the metasediments, which are made up of gneisses. Exposures are scanty and highly weathered. The rock types are biotites, gneisses, granite gneisses and in parts with subordinate migmatites. The contact between

the gneisses and metasediments are gradational, Dahomeyan-Birrimian in age (McCurry, 1970).

The Zaria crystalline rocks are part of the Nigerian Basement Complex. Oyawoye (1965) has shown that there is a structural relationship between this Basement Complex and the rest of the West African basement. This is partly due to the fact that the whole region was involved in a single set of orogenic episode, the Pan African orogeny, which left an imprint of structural similarity upon the rock units.

Granitic intrusions form a suite of batholiths (the Zaria Batholiths), part of which outcrops as the *Kufena* Hill. The gneisses are found as small belts within the granite intrusions, and are also found east and west of the batholiths. The biotite gneiss extends westwards to form a gradational boundary with the schist belt. The gneiss continues eastwards to some extent and is occasionally broken up by the Older Granite (McCurry, 1970). The Older Granite intrusion is supposed to have been formed at the bottom of a fold mountain belt (Wright and McCurry, 1970).

The thrusting imposed on the basement complex during the Pan African Orogeny movement is believed to have brought together rocks of different ages with different structural and metamorphic styles (Grant, 1969). The metasediment probably belongs to the sedimentary and granite facies that were formed in a geosynclinal trough which had earlier developed at the end of the Pan African Orogeny (Tokarski, 1972). During the Pan African Orogeny, the sediments and igneous material, together with the former metamorphosed basement rocks behaved as one tectonic unit. Some of these metamorphosed rocks became assimilated into the granite intrusions that accompanied the last orogeny (Grant, 1969).

Basement geology was affected by an orogeny, which predated the emplacement of the Older granite. During this event, deformation of the basement produced north-south trending basin of metasediment in the form of synclinoria (Trustwell and Cope, 1963). Tertiary east movement tilted the metasediments to the north and warped the basement along the axis of uplift (Russ, 1957). Two of the Russ' axes pass through the present Kaduna State having north-south trend and have a pronounced effect on the drainage of the state. Crystalline rocks of the Basement complex may be altered, jointed or fractured. The process of alteration may give rise to loose aggregates above fresh basement or sometimes may create a laterite cover and a clayey horizon above loose altered bedrock. Primary porosities of fresh basement rocks are very low and the rocks also have very low permeability due to the presence of a few pores that are normally interconnected.

1.5.1 Petrology of Shika

The rock types found in the basin are discussed as follows:

(i) Older Metasediments

These are believed to be Birrimian (>100 million years) in age and rock types include gneisses, which have suffered at least two episodes of tectono-metamorphic deformations resulting in widespread occurrences of migmatitic and granitic gneisses (McCurry, 1976). They occupy isoclinal belts within the crystalline rocks with a N-S trending. Hence, it is overlain by igneous and metamorphic rocks of variable undifferentiated biotite and biotite hornblende gneiss in parts of Zaria as schist (mica).

(ii) Older Granites

They are believed to have intruded the Nigerian Basement complex during the Eburnean and Lower Cambrian ages. The Eburnean granites are fine-grained granites that

represent a group of minor discordant intrusions of small aerial extent, occurring as dykes and irregular bodies. The group includes biotite and muscovite granite and adamebites. They are pale brown equigranular and usually foliated. Their contact with the later granite is complex but in some places degradational and in some places replaced by the later granite. Some of the rock types include aegerine augen granite, granodiorite granite, quartzdiorite, and porphyritic biotite granite.

(iii) Younger Granites

The younger granites are found essentially in the Jos-Plateau and it also appears northwest and southwest Nigeria. They are high-level discordant intrusions in the Basement complex. They are a group of anorogenic rocks of Jurassic age (170 – 160 million years). They are quite younger than the Older granite but have equivalent composition. The major tectonic event that took place in the Jos-Plateau around the Jurassic era resulted in the emplacement of the Younger Granite and the associated rock assemblage. Outcrops occur as large masses (stocks) and some as ring dykes. Members include rhyolites, syenites and gabbros (basin rocks).

The granitic rocks intrude into both the crystalline complex and the metasediments. The main petrographic units are porphyroblastic hornblende granite which are found in the extreme northern part and share boundary with the porphyroblastic biotite. The colour of the rock is dark green to brown and foliation is weakly defined. Porphyroblastic biotite granite is the commonest of the granitic rocks found in the area. It has a pink greyish colour and occupies southeast and central north part. Foliation is defined by the parallel alignment of feldspar and biotite. The megacrysts of feldspar are mainly microcline in composition. Pegmatites and aplites are found as

discordant or concordant veins within the host rock especially in the porphyroblastic granites in the southeast.

(iv) Gneiss

The gneissic complex is medium to coarse grained and are moderately to weakly foliated rocks. They are principally composed of quartz, oligoclase, biotite and occasionally porphyroblastic microcline (McCurry, 1970). The Older Granites are non-porphyroblastic and are variably foliated. They contain concordant biotite-rich segregation and are mainly composed of quartz, turbid oligoclase and accessory apatite (Trustwell and Cope, 1963).

(v) Schist

The schist is found as parallel lenses in the biotitic gneiss west of Ungwan Kubanni, in the stream valleys. The schist occurs in thin vertical sheets striking in the north-south direction. The schistose metasediment contains mainly biotite feldspar and quartz (Adamu, 1973). Quartzites are often associated and concordant with the schistose lenses. The general geology of the study area is shown in figure 1.3. This figure is the map of Zaria sheet 102.

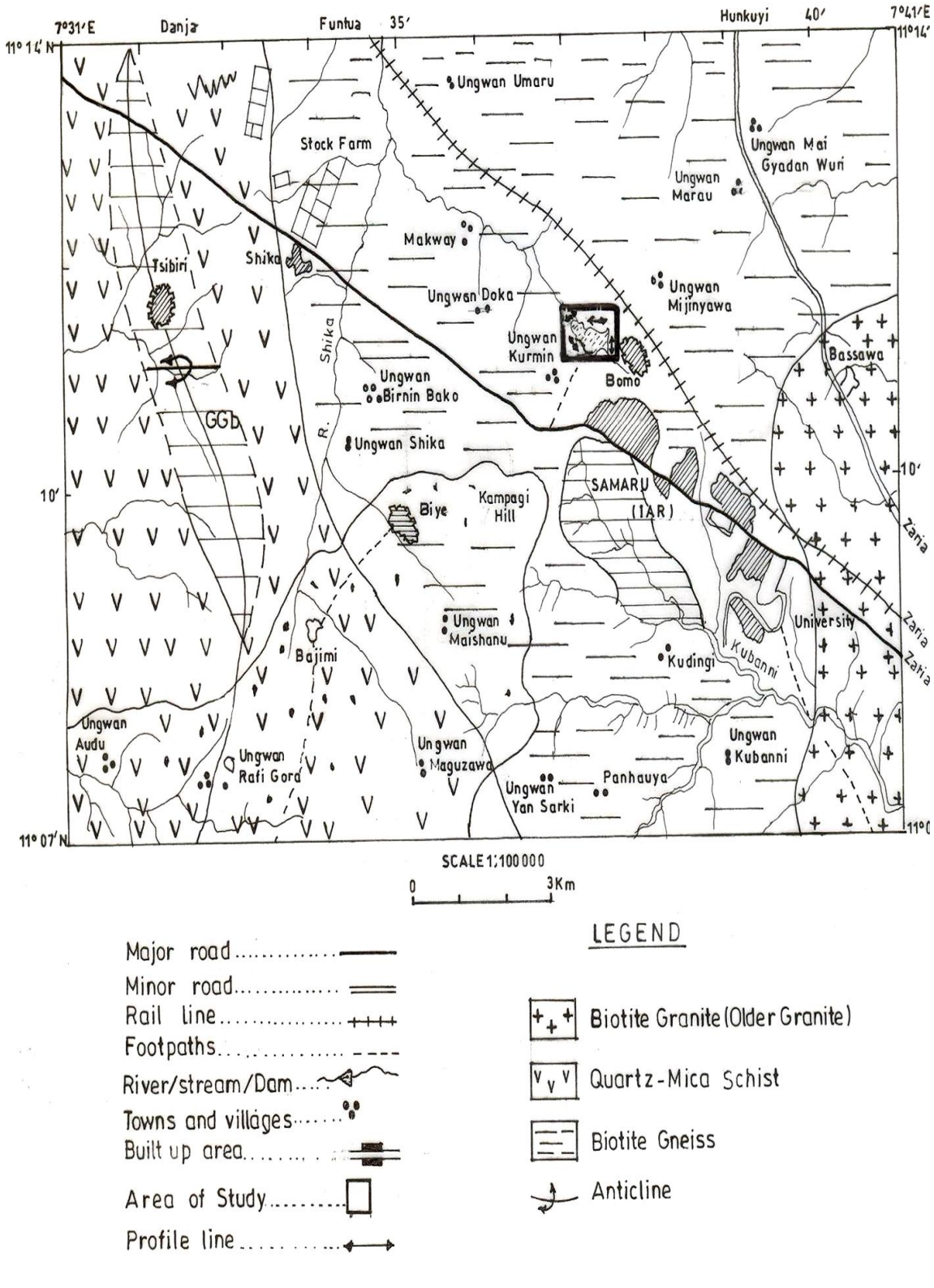

7°31'E
Danja
Funtua
35'
Hunkuyi
40'
7°41'E
11°14'N
Ungwan Umaru
Stock Farm
Ungwan Mai Gyadan Wuri
Ungwan Marau
Makway
Tsibiri
Shika
Ungwan Doka
Ungwan Mijinyawa
Ungwan Kurmin
Bomo
Bassawa
Ungwan Birnin Bako
R. Shika
GGD
Ungwan Shika
10'
SAMARU (IAR)
Kampagi Hill
Biye
Zaria
Ungwan Maishanu
University
Kubanni
Kudingi
Bajimi
Ungwan Audu
Ungwan Rafi Gora
Ungwan Maguzawa
Ungwan Kubanni
Ungwan Yan Sarki
Panhauya
11°07'N
SCALE 1:100000
0
3Km
LEGEND
Major road
Minor road
Rail line
Footpaths
River/stream/Dam
Towns and villages
Built up area
Area of Study
Profile line
Biotite Granite (Older Granite)
Quartz-Mica Schist
Biotite Gneiss
Anticline

Figure 1.3 Geological map of Zaria sheet 102.

1.6 Hydrogeology

Hydrogeology is often influenced by the climate, structure and geology of an area. This is because the geological formations underlying the area and their structures determine the type of aquifer to be encountered and the means of recharging them. The climate determines the water content and the rate of recharge of an aquifer. The climate and hydrological conditions control the surface and subsurface water in the area. The surface water is controlled by the underlying geology. Infiltration, evaporation, run off and overflow are the major factors responsible for groundwater recharge and accumulation (Umar, 2001).

Rainfall is the dominant factor that determines the occurrence of groundwater in the survey area. As such, this factor greatly affects the groundwater in the Shika. During the rainy season, Shika and its catchment area enjoy a fairly high amount of rainfall. Rainfall data for the last forty years show that the highest rainfall occurs in August while the lowest is in November. The average annual rainfall is about 1092mm (Olufemi, 1985). The higher the precipitation over an area, the greater the recharge. It has been observed that wells dug away from the river normally contain water at shallow depths. However, the water table falls progressively throughout the dry season. The amount of fall is determined by the location of the well from the river (Olowu, 1967). Generally, the closer a well is to the river channel, the smaller the fall. This fall is mainly controlled

by subsurface percolation of water into larger river valleys. Since the groundwater in the basin is unconfined, there are seasonal fluctuations in the water table (Olowu, 1967).

1.6.1 Types of Aquifer

The types of structures developed in the rocks also affect the occurrence of groundwater. Some rocks have pore-spaces, which are filled with water while others have dry pore spaces or none at all. In igneous rocks, porosity occurs primarily in the form of joints and fractures. Other non-crystalline rocks may be naturally highly permeable. The criteria that make formation a good aquifer include high effective porosity and permeability. These in turn depend on the degree of weathering and fracturing of the rocks.

The storage elements for groundwater in the Shika basin are described as follows:

(i) The Weathered Basement

Generally in this region, this is the most important aquifer. The thickness of this aquifer varies from place to place in the basin and is covered in most places by lateritic loam (Eigbefo, 1978). Wherever it is exposed to erosion, it exhibits evidence of mobilization (McCurry, 1970). Where the weathering of the rock has been in situ, which is mostly the case in this basin, the weathered product is usually capped by laterite.

(ii) The Laterite (Older Laterite) Deposits

These deposits contain little water. They are mostly unconsolidated and, because they are shallow, they receive direct recharge from rainfall. They are found all around the study area. They have varying thicknesses ranging from less than 1.0m to about 10.0m in some places in the basin, (Wright and McCurry, 1970).

(iii) The Alluvial Deposits

These consist of gravels, sands, silts and clay deposits. They are mostly found along the river channel and have thicknesses that vary from 5m – 15m (Olowu, 1967).

1.7 Previous Geophysical Study in the Area and its Environ

A geophysical investigation of the groundwater potential in the Institute for Agricultural Research (IAR) farm, Samaru, by Farouq Ado Umar, using ABEM Terrameter SAS 300 revealed that most parts of the area have three subsurface layers while some parts have two subsurface layers. The topsoil is sandy, clayey, silty, lateritic top soil with *fadama* loam except the farm sites under cultivation which are sandy and *fadama* loam. The weathered basement has variable depth ranging from 1m to about 16.6 m. Thickness of the weathered basement ranges from about 3.4 m to about 38.2 m. The fresh basement has a variable depth ranging from about 1.2 m to about 40 m. Thus the aquifer lies partly in the top soil and partly in the weathered basement, the thickest portion of the aquifer coinciding with the thickest portion of the weathered basement (Umar, 2001).

A resistivity survey in Jama'a village by Messrs Preussag Nigeria Limited with the aim of siting a borehole in the village has revealed the presence of faults within the bedrock, which have caused the downthrow of certain portions of the area (Umar, 2001). Borehole and pumping test data have been used previously to study the lithology, thicknesses of layers and aquifers. The study revealed three distinct layers which are, the overburden consisting of a top brownish red lateritic clay, about 9 m thick underlain by a brownish sandy clay soil, about 7 m thick. Underlying the overburden is the weathered basement composed of schistose rock materials, gravel and sand. The thickness is

variable, but usually 5 m – 14 m, (NWRI, 1&2, 2002). The fresh basement is a crystalline rock, mostly granite and schist and at a depth of 21 m – 40 m. Other works include preliminary investigation of groundwater condition in Zaria, geological mapping of the various rock types in and around Zaria, evaluation of the hydrogeological properties of the basin and the evaluation of groundwater for irrigation.

In a study of the surface water and its effect on groundwater in Zaria area, Olowu concluded that all streams, except the Galma River are seasonal, flowing only in the rainy season (Olowu, 1967). From his study of hydrogeological structures, which control groundwater flow in Samaru creek, Akpoborie concluded that structures like joints and fractures control groundwater flow the area occupied by the creek (Akpoborie, 1972). Also in a hydrogeological study of the basin, Eigbefo, concluded that the depth to water table at various points in the basin vary from about 3 m to about 10 m. He was also able to deduce that the thickness of the weathered basement aquifer within the basin ranges from about 1m to about 30 m (Eigbefo, 1978).

1.8 Aim and Objectives of the Survey

Since electrical images provide a detailed view (two-dimensional) of the subsurface structure, the present research study was designed to map a two-dimensional geoelectrical resistivity image of the study area for hydrogeological and geotechnical development.

Using the LUND Automatic Resistivity Imaging System produced by ABEM Instrument AB, the following objectives were achieved:

1. Determination of overburden thickness
2. Determination of the thickness of weathered basement

3. Determination of overburden layering or strata
4. Estimation of the groundwater potential (aquifer)

1.8.1 Scope and Limitations of the Survey

This research study covers only some parts of the permanent site of the Ahmadu Bello University Teaching Hospital (ABUTH), premises in Shika, Zaria.

There are several limitations to the inversion process. The program assumes 2D geometry or subsurface model, in which the resistivity remains constant perpendicular to the electrical resistivity imaging line. For the fact that two-dimensional algorithms are being used for interpretation, the subsurface structure must also approximate to two-dimension in a direction roughly perpendicular to the measured profile. Also, the program averages resistivity values over data blocks of different dimensions. The inversion algorithm favours images where neighbouring blocks have similar resistivity values. This procedure may cause the final inversion result to be smoothened (RES2DINV manual).

The data interpretation is affected by some combination of equivalence and suppression, the robustness of the algorithm and the number of layers used to model the data (Griffiths and Barker, 1993). Non-uniqueness of the inversion results poses a problem since it is possible for the calculated apparent resistivity values for slightly different models to be almost the same. Bad data points (unusually high or low apparent

resistivity) caused by instrumentation errors during the field survey, poor electrode contact, shorting of electrodes due to very wet conditions or metal objects (*e.g* fences, pipes *etc*.) or mistakes such as attaching electrodes to the wrong connectors are also pitfalls. The program allows for modification of some of the parameters such as the damping factor and the flatness filters which influence the inversion process (RES2DINV manual).

Another practical difficulty is the sensitivity of this method to minor variations in the resistivity of the near surface (i.e. near surface resistivity inhomogeneity). The practical difficulty in the field in dragging long cables and large number of electrodes over wooded or rugged terrain constitutes a problem. This is a slow and expensive task. Rugged topography constitutes a problem. The depth of penetration is Inverse Square limited. The method is suitable for outlining vertical contacts and horizontal beds but not usually suitable for irregularly shaped bodies or 3D bodies (Telford *et al*., 1990).

Another limitation of surface resistivity surveying is the decreasing resolution with depth. This is particularly so where no additional information, such as that provided by a borehole is available. Furthermore, for large depth penetration very large layouts are needed and the presence of conductive layers at the surface can still reduce the depth penetration of the method. However, one way to get high resolution at depth, and overcome depth limitations, is to carry out measurements with arrays of subsurface electrodes, often called resistivity tomography.

CHAPTER TWO

PRINCIPLES AND INSTRUMENTATION

We define tomography as an imaging technique, which generates a cross-sectional picture (tomogram) of an object by utilizing the object's response to the non-destructive, probing energy of an external source. Electrical resistivity tomography is a method by which 2D images of subsurface resistivity distribution are generated (Batayneh, 2006). Electrical Resistivity Imaging (tomography) involves measuring a series of constant separation traverses with the electrode spacing being increased with each successive traverse. Thus, 2D resistivity imaging requires data to be recorded with many different electrode separations along a line.

It is important to have a dense enough data to cover laterally and in terms of electrode separations to recover complex structures in the ground, which demands the use of automated multi-electrode data acquisition systems to be practical. The Wenner spread was used for this survey. The basis of the LUND Resistivity Imaging technique follows from that of the normal resistivity technique, in which case when a current is driven into the earth, any variation of the subsurface resistivity will alter the current flow, which will in turn affect the distribution of the electrical potential. Buried bodies distort the regular pattern of current flow.

A conductive body concentrates electric current flow lines towards itself while a resistive body causes the current to flow around itself. The potential fields are hence deflected and their deflections can be detected using potential electrodes at the surface of the earth. Thus, from the measurements on the earth's surface of the electrical potential and the current, it is usually possible to obtain information about the variation of the

subsurface resistivity. Because sand, fine grained sediments and bedrock are expected to exhibit large contrasts in electrical resistivity, the electrical resistivity method should be well suited to resolving them. When the resistivity values are correlated with differing types of geologic materials, they can provide useful information for interpretation.

2.1 Importance of Electrical Imaging

Electrical prospecting involves the detection of the surface effects produced by electrical current flow in the ground. A good number of electrical techniques are available because of the large variation in the conductivity of earth materials (rocks and minerals) describing the single property of earth material that varies over a wide range of the area. Thus, theoretically at least the resistivity methods are the most superior of all the electrical methods because quantitative results are obtained using a controlled source of specific dimensions (Telford *et al*., 1990). The applicability of the different resistivity methods supported by the ABEM Terrameter SAS 4000 is summarized in table 2.1.

Table 2.1 Applicability of Different Resistivity and Induced Polarization Methods. SP= Self Potential, VES= Vertical Electrical Sounding, Imaging= Profiling (with different electrode separations) and IP= Induced Polarization, (ABEM Terrameter SAS 4000 / SAS 1000 instruction manual).

Object of Search or Investigation	SP	VES	Imaging	IP
Archeological sites			*	
Cavities in the subsurface			*	
Clays, peat and soil	*		*	
Dam safety and leakage	*		*	
Groundwater in sedimentary areas		*		
Fracture zones in rock			*	
Groundwater in crystalline rock			*	
Groundwater/clay distinction				*
Groundwater flow	*			
Ores in hard rock areas	*		*	*

Overburden thickness		*		
Pollution of soil and groundwater			*	
Salt water invasion				*
Fissures in rock			*	

2.2 Theory

The electrical resistivity method is one of the most relevant geophysical methods applied for groundwater studies in basement terrains. In groundwater studies for instance, the relevance of the method is based on the usually significant resistivity contrast between the weathered zone and/or fractured column which contains the water and the resistive fresh bedrock.

There is a considerable variety of resistivity methods all of which employ artificial source of current which is introduced into the ground through point electrodes or long line contacts. The resulting potential established in the earth is measured at other electrodes in the vicinity of the current flow. The current is noted; hence it is possible to determine the apparent resistivity of the subsurface. In this regard, the resistivity method is the most superior; at least theoretically, to all other electrical methods since quantitative results can be obtained by using a controlled source of specific dimensions (Telford *et al*., 1990). Direct current or an alternating current of low frequency is used and the method is often called D.C. resistivity method.

In this method, an electric current is introduced into the ground by means of two current electrodes, which sets up a stationary current field, and because of the ohmic potential drop, an electrical potential field is also created. This field gets distorted in the neighbourhood of a subsurface zone of anomalous conductivity, and the aim is to search for such anomalous zones in the electrical field with a pair of potential electrodes. The assumption made here is that the current flow in the potential measuring circuit is negligible compared with the current flow in the ground, so that the potential electrodes

themselves will have no disturbing effect upon the electrical field (Grant and West, 1965).

The purpose of the Vertical Electrical Sounding method is to investigate the change of the formation resistivity with depth. To achieve this purpose it is necessary to arrange measurements, in such a way that, at each different measurement, the value of the measured potential difference is affected by the formation resistivity at a different depth range. This may be accomplished by changing the distance between the current electrodes so that the depth range to which the current penetrates is changed. However, the distance between the potential measuring electrodes and their position with respect to the current electrodes also affect the depth range from which information on the formation resistivity is obtained. The depth of penetration is proportional to the separation between the electrodes, in homogeneous ground, and varying the electrode separation provides information about the stratification of the ground.

The calculated quantity is called apparent resistivity, ρ_a. In the method employed in this study, Wenner Continuous Vertical Electrical Sounding (Wenner CVES) configuration was used. The electrode separation was 5m with the imager system using a multicore cable to which 41 electrodes were connected at takeouts moulded on at the predetermined equal intervals of 5 m. The interpretation of the Wenner CVES data is based on the assumption that the subsurface consists of a sequence of distinct layers of finite thickness and each of these layers is assumed to be electrically homogeneous and isotropic (Koefoed, 1979), and the boundary planes between subsequent layers are assumed to be horizontal. These assumptions in the real sense represent only a schematic description of the actual conditions that exist in the subsurface. There are some

deviations of the real subsurface conditions from the above assumptions, and these influence the Wenner CVES measurements and interpretation.

The Wenner CVES is based on the principle that the fraction of the electric current injected into the ground, penetrating below a given depth increases with the separation of current electrodes. Thus as the current electrode separation is increased, the depth of penetration will increase. Therefore, any anomalous body lying between the ground surface and the last depth of penetration will have great influence on the electrical potential field at depth.

Figure 2.1 shows the current and potential distribution within a homogeneous isotropic ground in a vertical plane through the current electrodes C_1 and C_2. When an external voltage is applied across them, there will be a flow of current through the earth from one electrode C_1 to the other, C_2. The resistivity method is based on measuring the potential between one electrode pair (P_1 and P_2, called potential electrodes) while transmitting DC between another electrode pair (C_1 and C_2) and r_1, r_2, r_3 and r_4 are the electrode separations. The rheostat varies the current I which is measured by the ammeter (A) while the voltmeter (V) measures the potential difference ΔU.

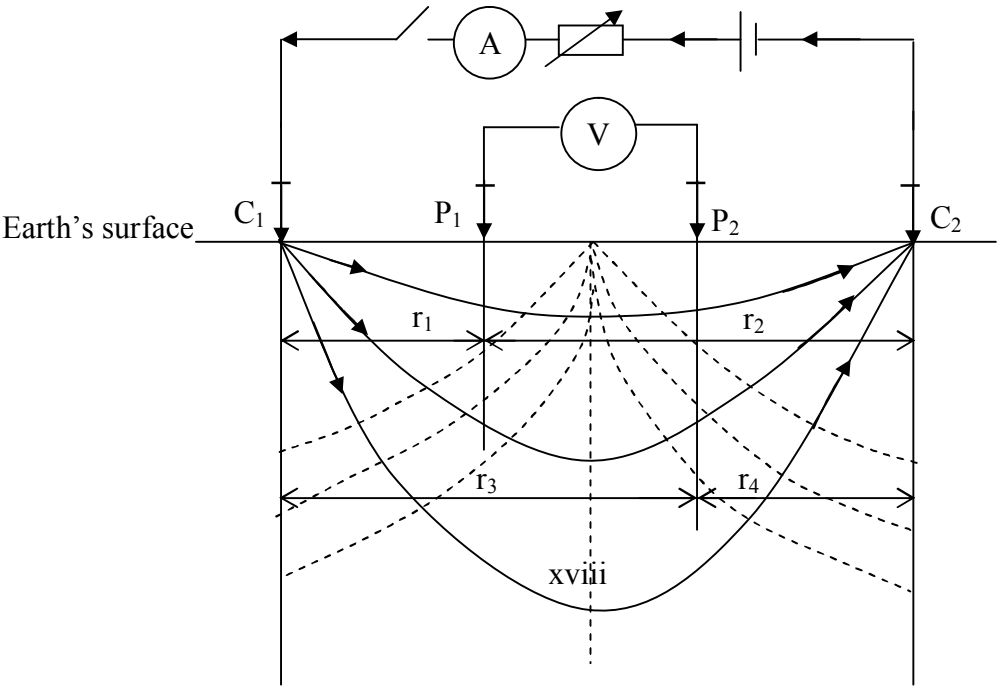


Figure 2.1 Current and Potential Distributions within Homogeneous Isotropic Ground.

The principle underlying the resistivity method is embodied in Ohm's law, which states that the current density at a given point is proportional to the electric field intensity at that point. Thus, Ohm's law gives the relationship between current density J (amperes/m^2) and electric field intensity E (in volts/m) as:

$$J = \sigma E \quad \text{---------- (2.1)}$$

The symbol σ is the conductivity of the medium. Also E is the gradient of a scalar potential U (in volts), *i.e.*,

$$E = -\nabla U \quad \text{---------- (2.2)}$$

Putting (2.2) into (2.1) gives

$$J = -\sigma \nabla U \quad \text{---------- (2.3)}$$

From divergence condition,

$$\nabla . J = 0 \quad \text{---------- (2.4)}$$

Thus, from (2.3)

$$\nabla . J = -\nabla . (\sigma \nabla U) = 0 \quad \text{---------- (2.5)}$$

Or

$$U\nabla^2 \sigma + \sigma \nabla^2 U = 0 \quad \text{---------- (2.6)}$$

Since σ is constant for a homogeneous medium, the first term in (2.6) vanishes hence,

$$\nabla^2 U = 0 \quad \text{---------- (2.7)}$$

Equation (2.7) is the so called Laplace's equation for a homogeneous earth. Applying boundary conditions, equation (2.7) can be solved for specific cases. For instance, for a single current electrode at the surface of a homogeneous ground, equation (2.7) can be expressed in spherical polar coordinates as:

$$\frac{1}{r^2}\frac{\partial}{\partial r}\left(r^2\frac{\partial U}{\partial r}\right)+\frac{1}{r^2\sin\theta}\frac{\partial}{\partial\theta}\left(\sin\theta\frac{\partial U}{\partial\theta}\right)+\frac{1}{r^2\sin^2\theta}\left(\frac{\partial^2 U}{\partial\phi^2}\right)=0 \quad \text{----} \quad (2.8)$$

For the current source, there is complete symmetry of current flow with respect to the θ and ϕ directions and the derivatives with respect to these directions are zero. Thus, equation (2.8) becomes

$$\frac{d}{dr}\left(r^2\frac{dU}{dr}\right)=0 \text{ ---------- (2.9)}$$

Equation (2.9) can be solved further to obtain

$$\mathrm{U}=\frac{I\rho}{2\pi}\left(\frac{1}{r}\right) \text{ ---------- (2.10)}$$

where ρ is the resistivity and I is the current.

Thus, the potential difference between two arbitrarily located points on the surface of a homogeneous isotropic ground with two point current electrodes on the ground's surface is given by the expression.

$$\Delta\mathrm{U}=\frac{I\rho}{2\pi}\left(\frac{1}{r_1}-\frac{1}{r_2}-\frac{1}{r_3}+\frac{1}{r_4}\right) \qquad \text{---------- (2.11)}$$

where r_1, r_2, r_3, and r_4, are the electrode separations as shown in Figure 2.1.

When the ground is not homogeneous ρ becomes ρ_a called the apparent resistivity and equation (2.11) can be written as:

$$\rho_a=\frac{\Delta U}{I}\frac{2\pi}{\left(\frac{1}{r_1}-\frac{1}{r_2}-\frac{1}{r_3}+\frac{1}{r_4}\right)} \text{ ---------- (2.12)}$$

The result is independent of the positions of the electrodes and is not affected when the current electrodes and the potential electrodes are interchanged.

The resistance R is calculated using Ohm's law:

$$R = \frac{\Delta U}{I} \qquad \text{---------- (2.13)}$$

Where R is the resistance in ohms; ΔU is the potential difference in volts; and I is the current in amperes.

The material parameter ρ, which is the inverse of electrical conductivity σ, is related to the resistance via a geometric factor K. The resistivity of the ground can be calculated using, the relation

$$\rho = K\,\frac{\Delta U}{I} \qquad \text{---------- (2.14)}$$

And $$K = \frac{2\pi}{\left(\frac{1}{r_1} - \frac{1}{r_2} - \frac{1}{r_3} + \frac{1}{r_4}\right)} \qquad \text{---------- (2.15)}$$

The Wenner spread (WEN32SX) CVES was adopted for this survey. Depth probes provide models of vertical variations in ground resistivity using an expanded electrode array offset from a central reference point. Depth penetration increases with wider electrode separation providing a 1D layered resistivity model. Composite sections are produced by interpolating between depth probes taken at regular intervals along a survey line. Resistivity imaging is an advanced development of the traditional resistivity surveying using four equally spaced electrodes set in standard configuration. Enhanced data quality and resolution provide continuous 2D resistivity models. Forty-two electrodes were used and unit electrode spacing is determined by parameters such as profile length, desired resolution and targeted depth of penetration.

A switching unit takes a series of constant separation readings along the entire length of the electrode array. The separation between sampled electrodes is then widened to increase the effective depth penetration. Electrodes are sequentially activated as either current or potential electrodes and apparent resistivities are determined for numerous overlapping electrode configurations. These numerous measurements along a line yield a distribution of apparent resistivities for the sub- surface. The apparent resistivities are then converted to true resistivity values using a numerical inversion that determines the best least-squares fit to the observed data with an objective function smoothing term that stabilizes the inversion.

2.3 Wenner Array

The Wenner spread is one of the most commonly used and presently the most popular array. This electrode array has one current electrode followed by two potential electrodes and ends with the second current electrode. The four electrodes are uniformly or equally spaced in a line (collinear), $r_1 = r_4 = a$, called the array spacing and $r_2 = r_3 = 2a$; thus the geometry is quite simple. Hence, geometric factor,

$K = 2\pi a$;

Apparent resistivity $\rho_a = 2\pi a \frac{U}{I} = K \frac{U}{I}$ ---------- (2.16)

The Wenner array was chosen for several reasons. It is a robust array in the presence of measurement noise. It is well suited to resolving horizontal structures because it is more sensitive to vertical changes in resistivity than to horizontal changes in resistivity. It covers an intermediate depth range, has intermediate resolution and shows sensitivity to geological noise. The number of measurements required to construct a

pseudosection is much smaller than with the other arrays. It has the highest signal-to-noise ratio among the conventional arrays of different electrode arrangements of the Wenner array shown in figure 2.2.

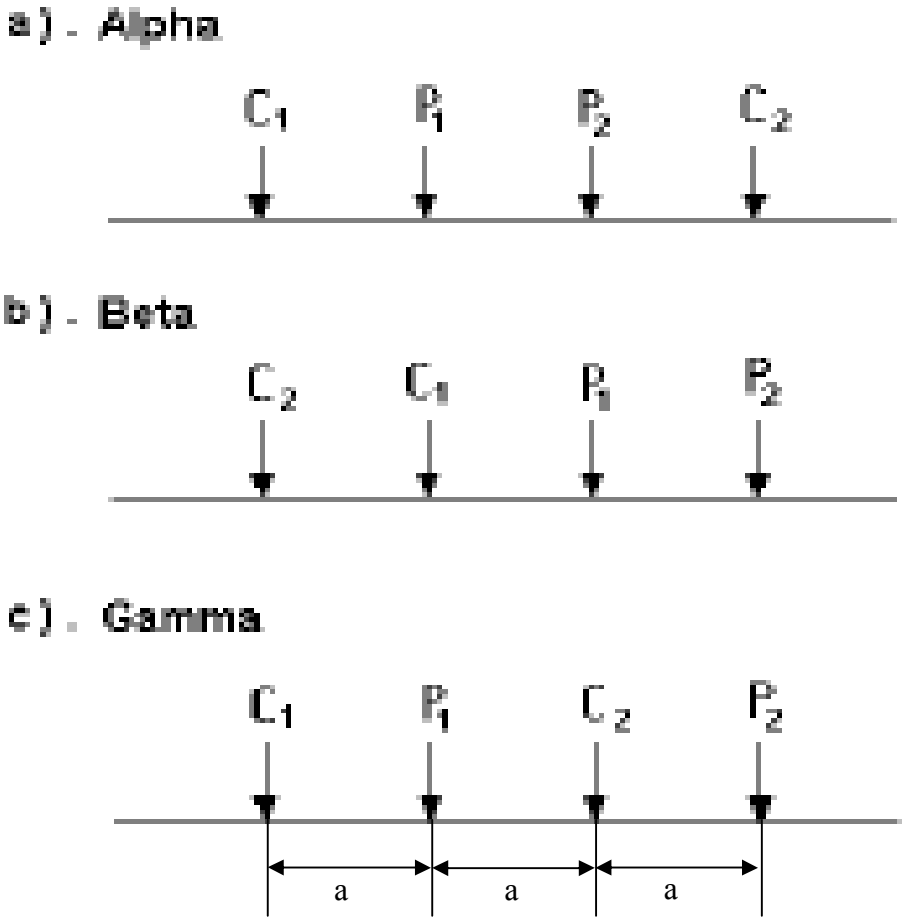


Figure 2.2 Wenner α, β, and γ Arrays showing Different Electrode Positions.

2.4 The Concept of Apparent Resistivity

Subsurface resistivity is measured by applying an electric current through two current electrodes and measuring the resulting voltage difference between potential

electrodes. For the general four electrode spread, the potential difference between the potential electrodes is given by equations 3.11, 3.12 and 3.14.

From equation 3.12, by measuring ΔU and I and knowing the electrode configuration, the resistivity can be calculated. Over uniform earth or homogeneous isotropic medium this calculated resistivity is constant for different electrode separation and any current. However, if the ground is inhomogeneous, the calculated resistivity varies as the electrode spacing is varied or the array is moved about. This calculated resistivity is called "apparent resistivity ρ_a", which is diagnostic of the real resistivities of the subsurface in the vicinity of the electrode array. The apparent resistivity may be smaller or larger than the real resistivities or in rare cases identical with one of the two resistivity values in a homogeneous surface. The apparent resistivity is the same as the real resistivity in a homogeneous subsurface, but normally a combination of contributing strata. The value of the apparent resistivity obtained with small electrode spacing is called the surface resistivity. This is equal to the true surface resistivity only if the ground is uniform over a volume roughly if the dimension of the electrode separation. In any layout the potential and current electrodes can be interchanged and by the principle of reciprocity, the apparent resistivity should be the same (unchanged) in either case.

2.5 Typical Resistivity Values of Earth Materials

Of all the physical properties of earth materials (rocks and minerals), electrical resistivity shows the greatest variation. Resistivity of metallic minerals may be as small as 10^{-5} Ωm, that of dry close-grained rocks like gabbro could be as large as 10^{7} Ωm. The maximum possible range is even greater, from native silver, 1.6×10^{-8} Ωm to pure sulphur 10^{16} Ωm. A conductor is usually defined as a material of resistivity less than 10^{-5} Ωm

while an insulator is one having a resistivity greater than 10^7 Ωm, between this limit lies the so-called semi-conductors (Telford *et al*., 1990).

The common minerals forming rocks and soils have very high resistivity in a dry condition and the resistivity of rocks and soils is therefore normally a function of the amount and quantity of water in pores and fractures. The degree of connection between cavities is also important; consequently the resistivity of a rock type or soil type may vary widely. The electrical resistivity varies between different geological materials depending mainly on variations in water content and dissolved ions in the water. Resistivity investigations can thus be used to identify zones with different electrical properties, which can then be referred to different geological strata. However, the variation may be limited within confined geological area and variations in resistivity within certain soil or rock type will reflect variations in physical properties.

For example the lowest resistivities encountered for sandstones and limestone mean that the pore spaces in the rock are saturated with water, whereas the highest values represent strongly consolidated sedimentary rock or dry rock above the groundwater surface. Sand, gravel and sedimentary rock may also have very low resistivities provided the pores in the rock are saturated with saline water. Fresh crystalline rock is highly resistive apart from certain ore minerals, but weathering commonly produces highly conductive clay rich saprolite. The variations in characteristics within one type of geological material makes it necessary to calibrate resistivity data against geologic documentation from for instance surface mapping, test pits or drilling. A typical range of resistivities of geologic materials is shown in figure 2.5.

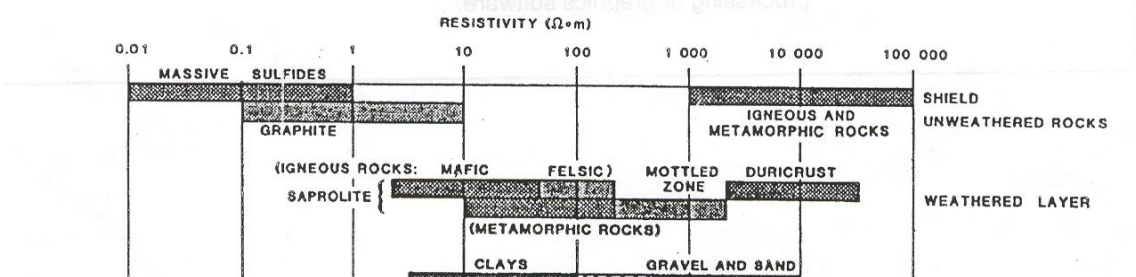


Figure 2.5 A Typical Range of Resistivities of Geological Materials (ABEM Instruction Manual).

The amount of water in a material depends on the porosity, which may be divided into primary and secondary porosity. Primary porosity consists of pore spaces between the mineral particles and occurs in soils and sedimentary rocks. Secondary porosity consists of fractures and weathered zones, and this is the most important porosity in crystalline rocks such as granites and gneisses. Secondary porosity may also be important in certain sedimentary rocks such as limestone. Even if the porosity is rather low, the electrical conduction taking place through water filled pore spaces may reduce the resistivity of the material drastically.

The degree of water saturation will of course affect the resistivity, thus the resistivity above the groundwater level will be higher than below if the material is the same. Consequently the method can be used to find the depth to groundwater in materials where a distinct groundwater table exists. However, if the content of fine grained material is significant, the water content above the groundwater surface, held by hygroscopic and capillary forces may be large enough to dominate the electrical behaviour of the material.

The resistivity of pore water is dominated by the concentration of ions in solution, the type of ions and the temperature. A range of resistivities for different types of water is given in table 2.2.

Table 2.2 Electrical resistivity of some kind of natural waters (ABEM instruction manual, LUND Imaging System).

TYPE OF WATER	RESISTIVITY (Ωm)
Precipitation	30 – 1000
Surface water in areas of igneous rock	30 – 500
Surface water in areas of sedimentary rock	10 – 100
Groundwater in areas of igneous rock	30 – 150
Groundwater in areas of sedimentary rock	>1
Sea water	≈ 0.2
Drinking water (maximum salt content 0.25%)	> 1.8
Water for irrigation and livestock watering (max. salt content 0.25%)	> 0.65

The presence of clay minerals strongly affects the resistivity of sediments and weathered rock. The clay minerals may be regarded as electrically conductive particles which can absorb and release ions and water molecules on its surface through an ion exchange process. Very roughly, igneous rocks have the highest resistivity, sedimentary rocks the lowest and metamorphic rocks intermediate. However, there is a considerable overlapping. Resistivities of particular rock types vary with age and lithology, since the porosity of the rock and the salinity of the contained water is affected by both. For example the resistivity range of Precambrian volcanic is 200 Ωm – 5000 Ωm while for quaternary rocks of the same kind it is 10 Ωm – 200 Ωm (Telford *et al*., 1990).

As the variation in temperature of ground is generally small, the temperature influence is normally negligible. However, in geothermal applications the variation could be significant even in permafrost regions. The mobility of ions increases with increasing

temperature as the viscosity of water is lowered. Hence, a decrease in resistivity with increasing temperature can be observed for materials where electrolytic conduction dominates.

2.6 Instrumentation

For resistivity measurement nowadays, there is a range of instrumentation from very simple to highly sophisticated equipment with the latter including the computer for infield data processing. The basic parts of any resistivity instrumentation are a portable power source which is either a D.C. or a low frequency A.C. Electrodes, preferably stainless steel electrodes and cable and reels, meters for measuring current and voltage both of which may be combined in a single meter reading resistance or apparent resistivity. With the development of computer-controlled data collection and also automatic data inversion, the use computer-controlled multi-electrode systems with automatic measurement and data quality control for the data acquisition which allow a dramatic increase in field productivity became very relevant. Such is the ABEM LUND Imaging System.

2.7 The ABEM Lund Imaging System

The LUND Imaging System is a multi-electrode system for cost effective and high resolution 2D and 3D resistivity surveys. It is an automatic electric imaging system suited for automatic resistivity profiling and drilling. The LUND Resistivity imaging System consists of a basic unit, a standard resistivity meter (ABEM Terrameter SAS 4000), a (4x64) multi-channel relay matrix switch unit called Electrode Selector ES 464. The system also has four multi-conductor electrode cables wound on reels each with 21

take-outs, stainless steel electrodes and cable jumpers and various connectors. The system is compatible with a portable PC-type computer or note book (laptop). Operating power comes from an internal 12 volts rechargeable NiCd battery pack. Data acquisition software featuring automatic measuring process, in-field quality control of measurements, automatic roll along, electrode cable geometry and switching sequence defined in address and protocol files which allows user defined survey strategies and arrays, onscreen echo of measurement progress, software for graphical and depth interpretation including pseudosection plotting in gray scale or colour, fully automatic 1D Zohdy depth interpretation of Wenner continuous vertical electric sounding (CVES). Model section plotting of 1D and 2D model interpretation sections in colour or gray scale including topography, reference data and reference levels, utility software for extraction of VES, data manipulation and conversion, graphical output in PCX-file format *etc*, are also available (ABEM instruction manual).

The Lund ES 464 basic system include one ES 464 field unit with clip-on NiCd rechargeable battery pack and one communication cable from electrode selector to Terrameter. It is light weight and has waterproof, rugged cast aluminium casing. The Terrameter SAS system consist of a basic unit called the Terrameter SAS 4000 and accessories like ES 464. SAS means Signal Averaging System. It is a method whereby consecutive readings are taken automatically and the results are averaged continuously. Signal Averaging System (SAS) results are more reliable than those obtained from single-short systems. The SAS 4000 can operate in different modes, *e.g.* resistivity, and self potential and induced polarization. In all its modes it is capable of measuring simultaneously in four channels thus making it suitable in all sorts of resistivity surveys.

The SAS 4000 is powered by a clip-on NiCd battery pack or by an external 12 volts source, which clips conveniently onto the bottom of the instrument. The SAS-EBA external 12 volts adapter allows the terrameter to utilize an external 12 volts D.C. source *e.g.* a car battery (ABEM LUND Instruction Manual).

Stainless steel electrodes establish electric contact between an electronic conductor, which are long cables, to an ionic conductor which is the ground. Electrodes generate noise, which is important only at the potential electrodes. Noise is the fluctuating voltage that appears between a pair of electrodes placed so close that no other natural voltages appear. But stainless steel electrodes create less noise. Current electrodes and potential electrodes make good contact with the ground to ensure low contact resistance and stability respectively (ABEM LUND Instruction Manual).

The cables incorporate heavy guage conductors with excellent insulation to ensure good survey results. The cables are expandable for deeper penetration by connecting them in series with a cable joint. The cables have take-outs at 5 m intervals along its length from which the cables are connected to the electrodes using cable jumpers having crocodile clips at both ends. The cables are wound on reels.

Figure 2.6 shows the basic instrumentation of the ABEM LUND Imaging System and accessories.



Figure 2.6 ABEM LUND Imaging System together with Terrameter SAS 4000 and ES 464 used for Electrical Resistivity Tomography.

CHAPTER THREE

METHODOLOGY

In geoelectrical resistivity tomography near-surface, a large number of electrodes are inserted into the ground and a computer-based system scans the whole array, thus realizing a combined sounding and profiling. If the target in a proposed survey area is narrow and extends over a long distance (the 2D case), the technique effectively investigates a series of depth ranges on a profile line, resulting in a pseudosection of apparent resistivities.

Tomographic surveys normally employ arrays of electrodes on the surface of the ground for data collection. The survey technique involves measuring a series of constant separation traverses with the electrode separation being increased with each successive traverse. Since increasing separation leads to information from greater depth, the measured apparent resistivities may be plotted as a contoured section, which reflects qualitatively the spatial variation in resistivity in the vertical cross-section. Length of profile, depth penetration and resolution required determine the unit electrode spacing.

3.1 Choice of the Method

Resistivity sounding is attractive as it is one of the cheapest geophysical techniques to employ and the measurements can normally be interpreted with low cost manual graphical methods. However with the increasing popularity of low cost portable computers, more effective techniques of electrical imaging are preferable. As a result of the successes recorded by the use of the electrical resistivity imaging/tomography technique in other parts of the globe, and in the crystalline basement areas of Bauchi State of Nigeria, the technique was adopted for this survey.

It is a common expectation that in-fill sediments or fractured rock show a high resistivity contrast with compact basement crystalline and structures, such as dikes, lava dooms, *etc*. This high resistivity contrast is considered to be a good target for electrical methods. The electrical resistivity tomography survey, as a non-destructive, cost effective method, has the additional advantage of rapid data collection and interpretation. Electrical resistivity imaging can provide much more meaningful and reliable data in the investigated ABUTH site.

3.2 Reconnaissance Survey

Topographical maps and geological maps were obtained. A walk around the entire area to be surveyed with these maps was made, to consider whether resistivity surveying was suitable for the current problem. It was discovered that the method was suitable. So possible profile lines were selected and the entire length of the planed profile lines inspected to ensure their practicability before returning to the area for the detailed survey.

3.3 Field Procedure

Electrical Resistivity Tomography (ERT) is a method by which 2D images of subsurface resistivity distribution are generated. Using this method features with electrical properties differing from those of the surrounding material may be located and characterized in terms of electrical resistivity, geometry and depth of burial. The electrical resistivity tomography data are collected using computer-controlled measurement systems connected to multi-electrode arrays. The data acquisition process is completely controlled by the computer software which checks that all the electrodes are

connected and properly grounded before measurement starts. After adequate grounding is achieved the software scans through the measurement *protocol* selected.

The WEN32SX CVES was chosen for this survey. The batteries of the Terrameter SAS 4000, Electrode Selector ES 464 were charged to full capacity before going to the field. Spare batteries were also taken along. Stainless steel electrodes, cable jumpers or electrode connectors, cable and reels, hammer, external 12 volts battery, a field umbrella, a measuring tape, 3 ranging poles, external battery adapter etc, were conveyed together with the members of the field team to the site of this research project, for commencement of the geophysical investigation.

The two electrode cables 1 and 2 depending on the current position along the line of survey were rolled out in the direction of the profile, with the cable reel end facing the highest coordinates. Each cable has 21 take-outs. As a rule the profiles were always running south-to-north or west-to-east to avoid confusion when the results are to be presented. The Terrameter SAS 4000 and the ES 464 were placed in the centre of the layout. The two cables were connected to the ES 464 at the centre of the cable spread. Take-out 1 and take-out 21 were made to overlap at the cable ends and in the layout centre. The serial port of the Terrameter was connected to the Electrode Selector. A booster was not used. The electrodes were connected to all the take-outs on intervals of 5 m on the electrode cables using cable jumpers. For a moist or soft ground electrodes were just pushed into the ground by hand and then connected. However, hammering and wetting was done on dry and hard ground.

For the long set-up, which was used on the field, a total of 41 electrodes were recognized because of the overlap of the 21st electrode of cable 1 with the 1st electrode of

cable 2 at the layout centre, which was recognized as a single electrode. The Terrameter was then connected to an external 12 volts battery and switched on, which automatically switches on the Electrode Selector and the system set-up which was echoed to the screen. The instrument was set to resistivity mode and LUND Imaging System was selected. A new file was created and a compatible *protocol* WEN32SX, *electrode separation* of 5 m, *cycles* 3, *range* = Ω, *current* = 20 mA, *maximum stack* = 3, were selected appropriately. The battery voltage was also checked, it was 12 volts.

Electrode test was commenced immediately, and grounding improved for the electrodes with bad ground contact. The connectors were also checked for unsatisfactory electrode positions.

Electrodes are tested pair-wise against each other starting from the outermost electrodes going toward the centre. The electrode test checks if it is possible to transmit current through all electrodes. This test takes a couple of minutes but saves time afterwards; because program may stop depending on poor electrode contact. Measurement may also stop if the batteries for either the Terrameter or the Electrode Selector are low. The program automatically continues to measure using the two electrode cables when the contact is satisfactory.

It was ensured that measurements have not stopped during the measurement period. As measurement continues apparent resistivity values are echoed on the screen. When measuring on each layout is finished the program was quitted and the Terrameter switched off. The cables were disconnected, wound up, and the electrodes and cable jumpers were all collected together. The instrument was then transferred to a new profile

and the entire process repeated until all the profiles were completed. The maximum number of data points was 190 per profile.

While measuring the profiles, the positions of reference points along the lines were noted. The used midpoints along the profiles were noted to facilitate identification of points for further investigation. A total of six profiles were taken (figure 1.1), and the centre of spread of profile 4 corresponded with the location of a borehole on the site. There are also boreholes within the hostels. A diagram of the field layout of the WEN32SX CVES spread is shown in figure 3.1.

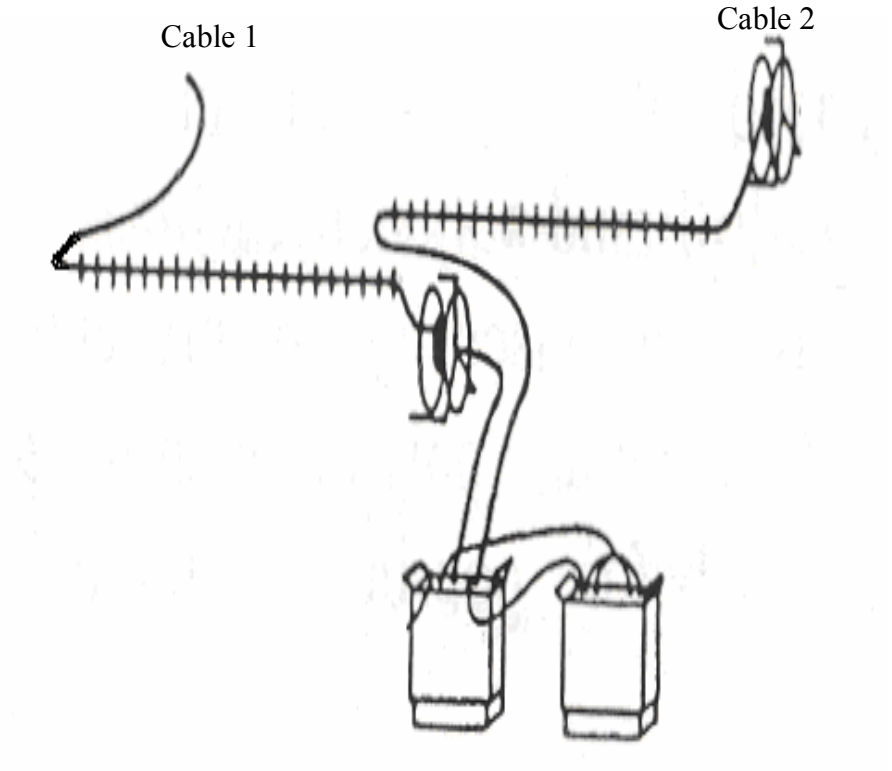


Figure 3.1 Typical Electrode Layout of WEN32SX: Wenner CVES with two cables using the Terrameter SAS 4000 and ES 464 in LUND Imaging.

The Electrode Selector ES464 does not put any restrictions on how to combine all the available channels. Electrode take-out spacing was set at 5.0m before starting data acquisition and this is used to calculate electrode positions, apparent resistivities and new station coordinates. Electrodes are sequentially activated as either current or potential electrodes, and apparent resistivities are determined for numerous overlapping electrode configurations (Meads *et al*., 2003).

3.4 Pseudosection Plotting

To obtain a good 2-D picture of the subsurface, the coverage of the measurements must be 2-D as well. As an example, Fig. 3.2 shows a possible sequence of measurements for the Wenner array for a system with 20 electrodes. In this example, the spacing between adjacent electrodes is "a". The first step is to make all the possible measurements with the Wenner array with electrode spacing of "1a". For the first measurement, electrodes number 1, 2, 3 and 4 are used. Notice that electrode 1 is used as the first current electrode C_1, electrode 2 as the first potential electrode P_1, electrode 3 as the second potential electrode P_2 and electrode 4 as the second current electrode C_2. For the second measurement, electrodes number 2, 3, 4 and 5 are used for C_1, P_1, P_2 and C_2 respectively. This is repeated down the line of electrodes until electrodes 17, 18, 19 and 20 are used for the last measurement with "1a" spacing.

After completing the sequence of measurements with "1a" spacing, the next sequence of measurements with "2a" electrode spacing is made. First electrodes 1, 3, 5 and 7 are used for the first measurements. The electrodes are chosen so that the spacing between adjacent electrodes is "2a". For the second measurement, electrodes 2, 4, 6, and

8 are used. This process is repeated down the line until electrodes 14, 16, 18 and 20 are used for the last measurement with spacing "2a" for a system with 20 electrodes.

The same process is repeated for measurements using "3a", "4a" *etc,* electrode spacing. To get the best results, the measurements in a field survey should be carried out in a systematic manner so that, as far as possible, all the possible measurements are made. This will affect the quality of the interpretation model obtained from the inversion of the apparent resistivity measurements (Dahlin and Loke, 1998).

Note that as the electrode spacing increases, the number of measurements decreases. The number of the measurements that can be obtained for each electrode spacing, for a given number of electrodes along the survey line, depends on the type of array used. The Wenner array gives the smallest number of possible measurements compared to the other common arrays that are used in 2-D surveys. A diagram of the sequence of measurement to build up a pseudosection is shown in figure 3. 2.

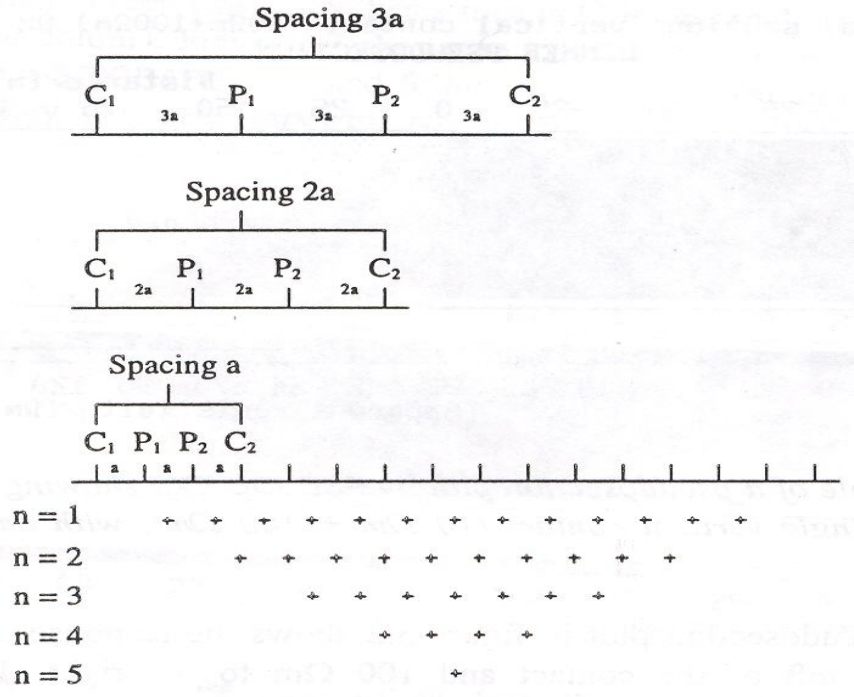


Figure 3.2 Principle for building up a pseudosection (ABEM instruction manual).

CHAPTER FOUR

FIELD RESULTS AND INTERPRETATION

Hydrogeological, environmental and civil engineering studies are increasingly demanding more precise and more detailed geoelectrical information at shallow depth. In order to make this cost effective and to compete with shallow, relatively inexpensive drilling, optimal use must be made of digital techniques, both in the acquisition and in the processing of field data (Overmeeren van, 1988). As electrical resistivity tomography (ERT) is an ill-posed problem, *a priori* information about unknown parameters (such as resistivity values and depth of the layers) are of paramount importance for inversion processing (Cardarelli, 2006).

As in all other geophysical methods, the interpretation of data from electrical imaging involves expressing in geological terms the information obtained from the measured apparent resistivity data. Such an interpretation demands, on the one hand, considerable practical experience with the method and, on the other hand, a sound knowledge of the geology of the region under consideration.

An automatic iterative method based on the smoothness-constrained least-squares method; known as RES2DINV was used. This rapid 2D resistivity inversion routine considerably sharpens up the image, places the structures at approximately their correct depths and provides acceptable estimates of their true resistivities. In this work, all the available geological information on the project area was taken into consideration to constrain the interpretations. Also in interpreting the data, each layer of rock type was assumed to be homogeneous and isotropic.

4.1 Data Processing

The raw field data were processed using RES2DINV (Loke and Barker, 1996). This is a computer program that automatically determines a two-dimensional (2D) resistivity model for the subsurface for the data obtained from electrical survey. It is a Window based program. This method is based on the following equation

$$(\mathbf{J}^T\mathbf{J} + u\mathbf{F})\mathbf{d} = \mathbf{J}^T\mathbf{g} \quad \ldots\ldots\ldots\ldots\ldots\ldots\ldots\ldots\ldots\ldots\ldots\ldots\ldots\ldots\ldots\ldots 3.1$$

Where $\mathbf{F} = \mathbf{f}_x\mathbf{f}_x^T + \mathbf{f}_z\mathbf{f}_z^T$

$\mathbf{f}_x$ = horizontal flatness filter

$\mathbf{f}_z$ = vertical flatness filter

$\mathbf{J}$ = matrix of partial derivatives

u = damping factor

$\mathbf{d}$ = model perturbation factor

$\mathbf{g}$ = discrepancy vector

The *forward problem* is solved through a finite difference algorithm, whose main features are a versatile user-defined discretization of the domain and a new approach to the solution of the inverse Fourier transform. The forward modelling subroutine is used to calculate the apparent resistivity values. The *inverse procedure* is based on an iterative smoothness-constrained least-squares algorithm. This computer program uses a smoothness constrained non-linear least-squares optimisation inversion technique to convert measured apparent resistivity values to true resistivity values and plot them in cross-sections.

The inversion process removes geometrical effects from the pseudosection and produces an image of true depth and true formation resistivity. One advantage of this method is that the damping factor and flatness filter can be adjusted to suit different types of data. The program creates a resistivity cross-section, calculates the apparent resistivities for that cross-section, and compares the calculated apparent resistivities to the measured apparent resistivities. The iteration continues until a combined smoothness constrained objective function is minimized. The depth of investigation cannot be determined by simple calculations and it depends on the acquisition geometry, the conductivity structures and data errors (Oldenburg and Li, 1999). However, they demonstrated through various modeling exercises that there is a loss of reliability in the inverted resistivity values at the bottom and ends of resistivity images where the resistivity values are least constrained by the data.

A common method for presentation of CVES and 2D resistivity data is the drawing of pseudosections. A pseudosection is made by plotting the data points in a diagram, using the length axis for the distance along the surveying line and the depth axis for the electrode separations, (ABEM Instruction Manual), as indicated in Figure 3.2. The distance for the electrode configuration midpoint is thus plotted against the electrode separation for each measured data point, letting the latter reflect the measurement depth. The corresponding apparent resistivities for the plotted points are then used to contour the variation in apparent resistivity along the surveying line. The pseudosection thus obtained reflects the variation of resistivity in the ground in a qualitative way, and approximate structures and depths to layer interfaces may be estimated. It should be noted that the pseudosection is simply a 2D equivalent of the plotted field data points in a linear depth

scale. In this context, drawing of pseudosections needs computer assistance to be practical due to the large amount of data.

The PSEUDO.EXE and ERIGRAPH.EXE software are developed for automatic drawing of pseudosections in grey scales or colours, using linear interpolation between data points. Linear interpolation involves no smoothing of data, which gives a good indication on the data quality. Twelve different colours or grey levels are used for plotting data. Each data point used for drawing the pseudosection is indicated in the section by a dot. Presenting DC-resistivity data in colour plots may be disputable as the data does not contain any spectral information. However, presenting D.C. resistivity data in colour plots makes it easier to see the variations in resistivity, which is important as small changes in resistivity in one part of a long profile may be significant even if there is a very large variation along the profile. The selection of resistivity interval limit is of major importance when presenting data, as the perception of the plotted data is strongly controlled by the colours. A suitable selection of limits enhances the geological variation while unsuitable selection of limits may hide important information or enhance irrelevant features. A geological reference was used to optimize the data presentation.

The program was developed for plotting of DC-resistivity data measured with a multi-electrode array, implying electrode spacings are always an integer multiple of the smallest electrode spacing used. Furthermore, profile distance coordinates are assumed to fall into the same positions as data for the smallest electrode spacings or halfway between them. For long profiles the data matrix used for the interpolation routine will not be sufficient for plotting the whole profile at once. In cases where the data does not fit, it is automatically divided into small enough portions for the interpolation routine, and plotted

one portion after the other in the same section. In this way there is no limit to the number of data points in the direction along the profile. There is however, a limit to the number of data points in the depth direction, which depends on the array size specified before compiling the program, but for DC-resistivity data the number of different electrode spacings is normally very limited.

The 2D model used by the program divides the subsurface into a number of rectangular blocks, to determine the resistivity of the rectangular blocks that will provide an apparent resistivity pseudosection that agrees with the actual measurements. For the Wenner and Schlumberger arrays, the thickness of the first layer of blocks is set at half times the electrode spacing. The arrangement of the blocks is loosely tied to the distribution of the data points in the pseudosection. The distribution and the size of the blocks is automatically generated by the program, so that the number of blocks usually do not exceed the number of data points. The depth of the bottom row is set to be approximately equal to the equivalent depth of investigation of the data points with the largest electrode spacing. This arrangement is shown in figure 4.1.

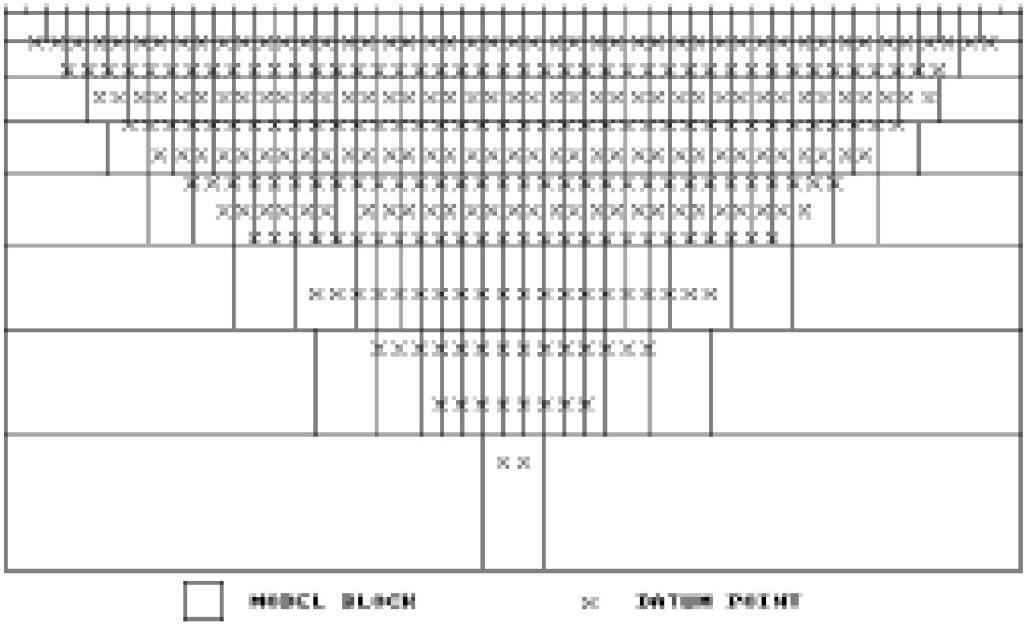


Figure 4.1 Arrangement of the blocks used in a model together with the datum points in the pseudosection (RES2DINV).

4.2 Interpretation Technique

Interpreting the resistivity data consists of two steps: a physical interpretation of the measured data, resulting in a physical model, and a geological interpretation of the resulting physical parameters (Dahlin, 2001). The large-scale VES data were interpreted with the state-of-the-art interpretation technique, called the 2D smoothed damped least-squares inversion algorithm. The results obtained based on 2D inversion of field data and borehole information, were interpreted to determine the depth and extent of shallow bedrock, thickness of overburden, aquifer *etc*. In interpreting LUND Imaging data, Computer assistance is needed due to the large amount of data collected from the field. The PSEUDO.EXE and ERIGRAPH.EXE software for instance are developed for automatic drawing of pseudosections in grey scales or colour, using linear interpolating between data points. Third party software packages for resistivity data processing can also be used for advanced interpretation. One example of such a program is RES2DINV.EXE, which performs smoothness constrained inversion (automatic model interpretation) using finite difference forward modelling and quasi-Newton techniques (Loke, 1994).

The true resistivity structure was interpreted using automatic 2D smoothness constrained least-squares inversion. The smoothness constrain prevents unstable and

extreme solutions, whereas a quasi-Newton reduces the numerical calculations (Loke and Barker, 1996). Quite often a useful amount of information can be extracted from a pseudosection by careful inspection of the contour pattern and apparent resistivity values, particularly if some geological control is available. Contours tend to follow horizontal or gently sloping boundaries between strata of different resistivities, though steep contacts are much smoothed. Such steep boundaries provided they show a strong resistivity contrast can be identified using some of the gradient measure. Contour peaks and troughs are correctly positioned relative to the subsurface features giving rise to them, and some estimate of depths at which boundaries occur may be made.

Hence, qualitatively speaking, the subsurface structure may be quite obvious though this is by no means always so. If there are marked departures from 'two-dimensionality,' the contour pattern may be affected by resistivity contrasts close to, but outside the plane of the section. Such effects can lead to serious errors both at the qualitative and quantitative stages of interpretation. Also faulting can be difficult to detect due to the smoothing effect of the Wenner array (Griffiths *et al.*, 1990). Even if the acquisition of a data set is straightforward due to the improvements in resistivity devices, the interpretation involves many factors and can be difficult when some parameters in the inversion procedure are neglected. Such parameters include the stability, robustness and uniqueness of the inversion algorithm (Cardarelli, 2006).

4.3 Geological Control

A good knowledge and use of the geology of an area is very important for any meaningful interpretation of any geophysical data collected from the area. Therefore, in this work, information obtained from previous works and borehole logs within and close

to the area of survey was taken into consideration in the course of interpretation. These borehole logs were discussed elaborately in section 4.5.

4.4 Field Results

Two-dimensional electrical resistivity surveying can form a powerful geological mapping tool for use in engineering and environmental applications, including hydrogeological mapping. In combination with a limited number of drilling reference points, with locations based on the resistivity results, reliable models of the subsurface can be created (Dahlin, 1996). The field data (pseudosections) are inverted to produce models representing subsurface electrical resistivities. In cases where resistivity contrast is gradual, smooth inversion is more suitable, while when there is a sharp variation in resistivity contrast, block inversion is preferable (Cardarelli, 2006).

Mathematical parameters, such as damping factors and the smoothness matrix were checked and changed appropriately. Furthermore, modifying the inversion results by changing the starting model appears to be the best way to obtain the valid physical results from the inversion.

The optimization method basically tries to reduce the difference between the calculated and measured apparent resistivity values by adjusting the resistivity of the model blocks. An initial (starting) model, which is generated automatically by the program, is then modified to reduce the differences between the model response and the measured data. A measure of this difference is given by the Root-Mean-Square (RMS) error. This process continues iteratively until the RMS error is reduced to an acceptable limit. However, the model with the lowest possible RMS error is usually chosen, but can sometimes show large and unrealistic variations in the model resistivity values and might

not be the best model from a geological perspective. The most prudent approach is to choose the model at the iteration after which the RMS error does not change significantly (RES2DINV; Batayneh, 2006).

The electrical images along the profiles and their interpretation are discussed in this section. A total of six profiles were taken for this survey. Three of them, profiles 1, 2 and 4 are north-south trending while profiles 3, 5 and 6 are west-east trending. Profiles 1 and 2 are parallel to each other with profile 3 perpendicular to them. Profiles 5 and 6 are also parallel with profile 4 perpendicular to them. The profiles are indicated on the map of the study area (see figure 1.2). The inversion result for each profile is shown in figures 4.2 to 4.7 showing the images of the pseudosections (geoelectric sections) obtained from the processed data. The results show three distinct images for each profile. The upper image labelled (a) is a plot of the measured apparent resistivity pseudosection. The middle image labelled (b) is the calculated apparent resistivity pseudosection and the lower image labelled (c) is the true resistivity model obtained after a definite number of iterations of the inversion program. Borehole log is also superimposed on the inverse model for easy correlation. This description is applicable to all the results shown in figures 4.2 to 4.7.

Figure 4.2 shows the resistivity inversion results (iteration 8, 10.2% total average RMS error), for profile 1. Thus indicating that good fits between the measured (observed) and calculated apparent resistivity data were achieved. The robust data inversion option was used to remove the effect of a few data points that might be more noisy in the inversion results and the robust model inversion option was also used. Apparent resistivity (in ohm-metre, Ωm) is plotted against pseudo-depth (Ps.Z, in metres, m), but

with colour infill instead of line contours. A thick layer of very high resistivity (194 Ωm - 1223 Ωm) is observed along the top of the resistivity image. This correlates with the observed dry and consolidated lateritic clay top soil with gravel and sand. This layer constitutes the overburden, which is about 10.8 m thick. The disintegrated schistose, sandy, silt, clay, and gravel channels that run through the cross-section correspond with the resistivity values (30.8 Ωm – 487 Ωm). This is the fractured, saturated and highly weathered basement consisting of aquiferous sand and gravel. Here the aquifer is a low resistivity weathered material. Although fractures are not directly indicated, the increased thickness of weathering here provides a good reservoir. The zone of significantly lower resistivities (<1.96 Ωm - >12.3 Ωm) in the inverse model indicates a zone of fracturing and weathering. This has a thickness of about 10 m at a depth of about 8 m from the surface and extends between the 80 m and 140 m marks. There is a high probability of bedrock fracturing. The depth to bedrock is greater than 30 m. This pseudosection correlated well with the borehole logs obtained from the Preussag Ltd and ABUTH hostels, as shown in figures 4.8 and 4.10 of section 4.5.

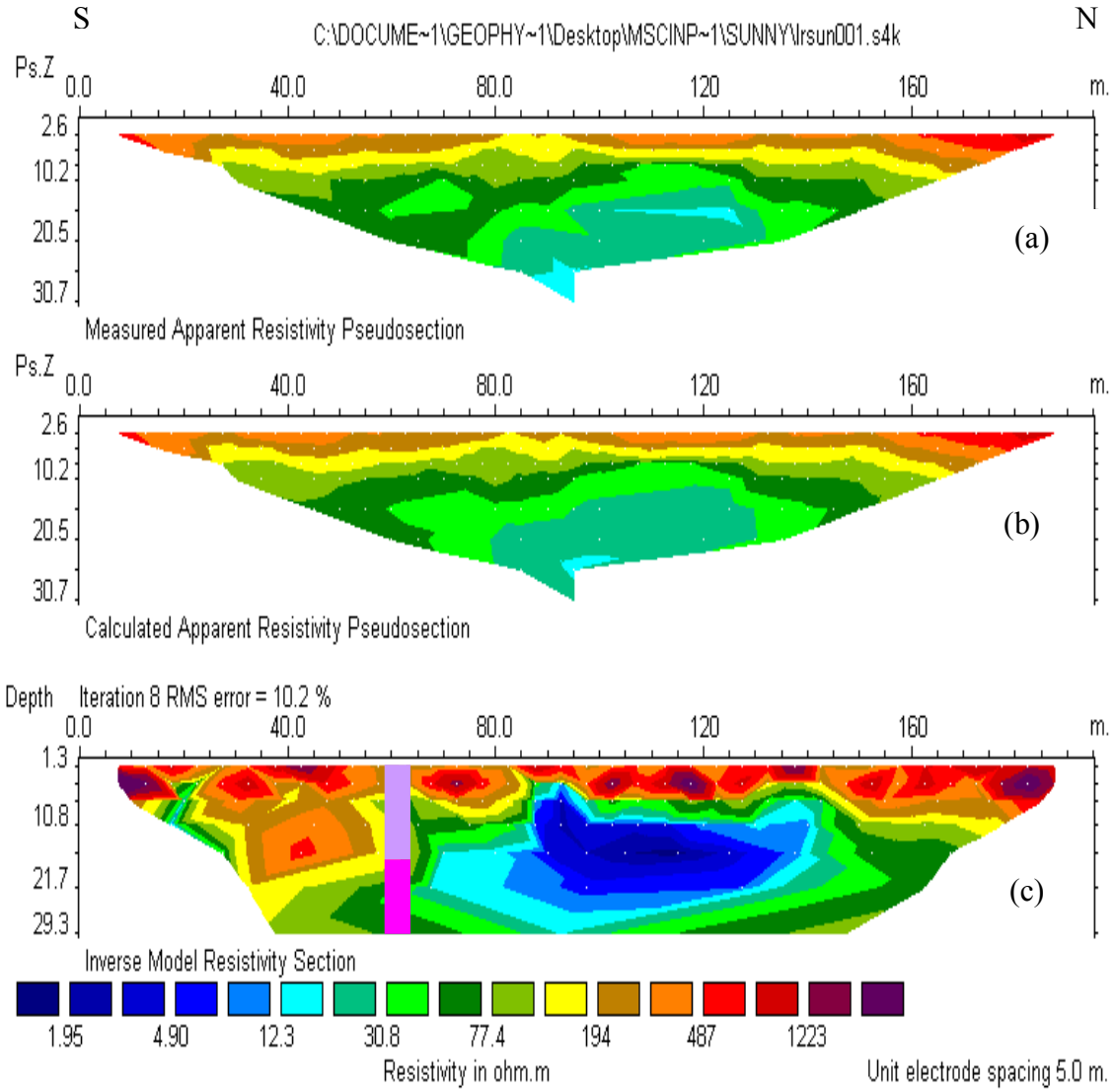


Figure 4.2 The result of 2D inversion of the Wenner-array data along survey line 1, in the ABUTH hostel: (a) is the observed data plotted as a Pseudosection; Ps.Z = pseudo-depth. (b) is the calculated Pseudosection and (c) is the inverse model showing true depth and true formation resistivity. The thin vertical section is a borehole log superimposed on the inverse model for easy correlation.

Figure 4.3 shows the resistivity inversion results (iteration 9, 7.6 % total average RMS error), for profile 2. Thus indicating that good fits between the measured (observed)

and calculated apparent resistivity data were achieved. Both the robust data inversion option and the robust model inversion options were used in the inversion of the data set. The top layer is composed of consolidated laterite, gravel, sand, silt and clay having a high resistivity range of 216 Ωm - 684 Ωm. This is the overburden or the first layer having a thickness of about 15 m. Between 100 m and 130 m marks a high resistivity greater than >2162 Ωm is observed in the overburden and its due to a dry, empty suck-away pit (septic tank) that was tiled.

The weathered bedrock clearly shows on the image immediately underneath the overburden with a resistivity range of about < 21.7 Ωm - > 216 Ωm. It is made up of gravel, sand and other weathered rock materials. Between 120 m – 160 m marks a low resistivity (0.687 Ωm - > 6.86 Ωm) section is observed to be at a depth of 21.7 m from the surface. This is probably a highly fractured and weathered zone containing clayey deposit trapped in the aquifer. Patches of high resistivity material are observed at 40 m, 70 m and 160 m marks and are probably a crystalline rock or possibly corestones or unweathered bedrock at depth less than 10 m from the surface. The basement is shown by the image, by the high resistivity of 2162 Ωm and is believed to be at a depth greater than 21.7 m. This suggests increased bedrock weathering and fracturing and possibly the presence of fractures in the bedrock. This Pseudosection correlated well with the borehole logs obtained from Shika main town, as shown in figure 4.9 of section 4.5.

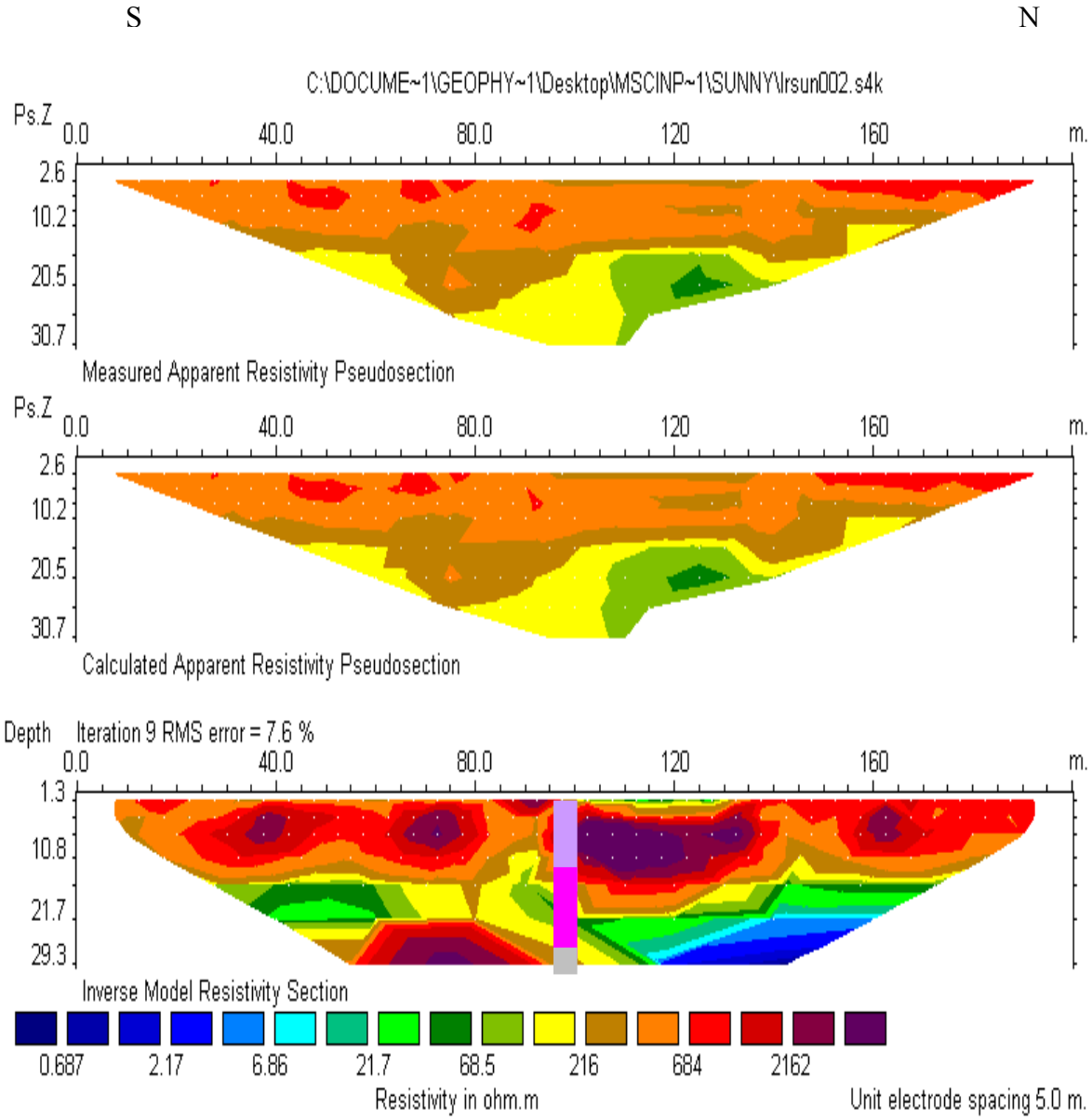


Figure 4.3 The result of 2D inversion of the Wenner-array data along survey line 2, in the ABUTH hostel.

Figure 4.4 shows the resistivity inversion results (iteration 5, 3.5% total average RMS error), for profile 3. Thus indicating that good fits between the measured (observed) and calculated apparent resistivity data were achieved. High resistivity (815 Ωm - >1408 Ωm) weathered material of thickness less than 15.0m, which is composed of consolidated laterite, gravel, sand; clay and silt formed the overburden. Patches of unweathered bedrock (>2435 Ωm), embedded in the consolidated laterite clearly shows below the 40 m, 90 m 110 m and 170 m marks and are close to the surface, at a depth less than 10 m. This layer overlay a low resistivity (<158 Ωm - >815 Ωm) aquifer at a depth of about 15 m from the surface. This layer is composed of gravely sand and disintegrated schistose materials. There is a much lower resistivity (52.8 Ωm - 158 Ωm) channel which is probably a fracture zone in the bedrock, and containing water. This is seen at a depth of about 21.7 m and rising to the surface below the 140 m mark. The increased thickness of weathering here provides a good reservoir with a higher probability of bedrock fracturing. The fresh basement is at a depth greater than 30 m as shown in the image. This pseudosection correlated well with the borehole logs obtained from the Preussag Ltd and ABUTH hostels, as shown in figures 4.8 and 4.10 of section 4.5.

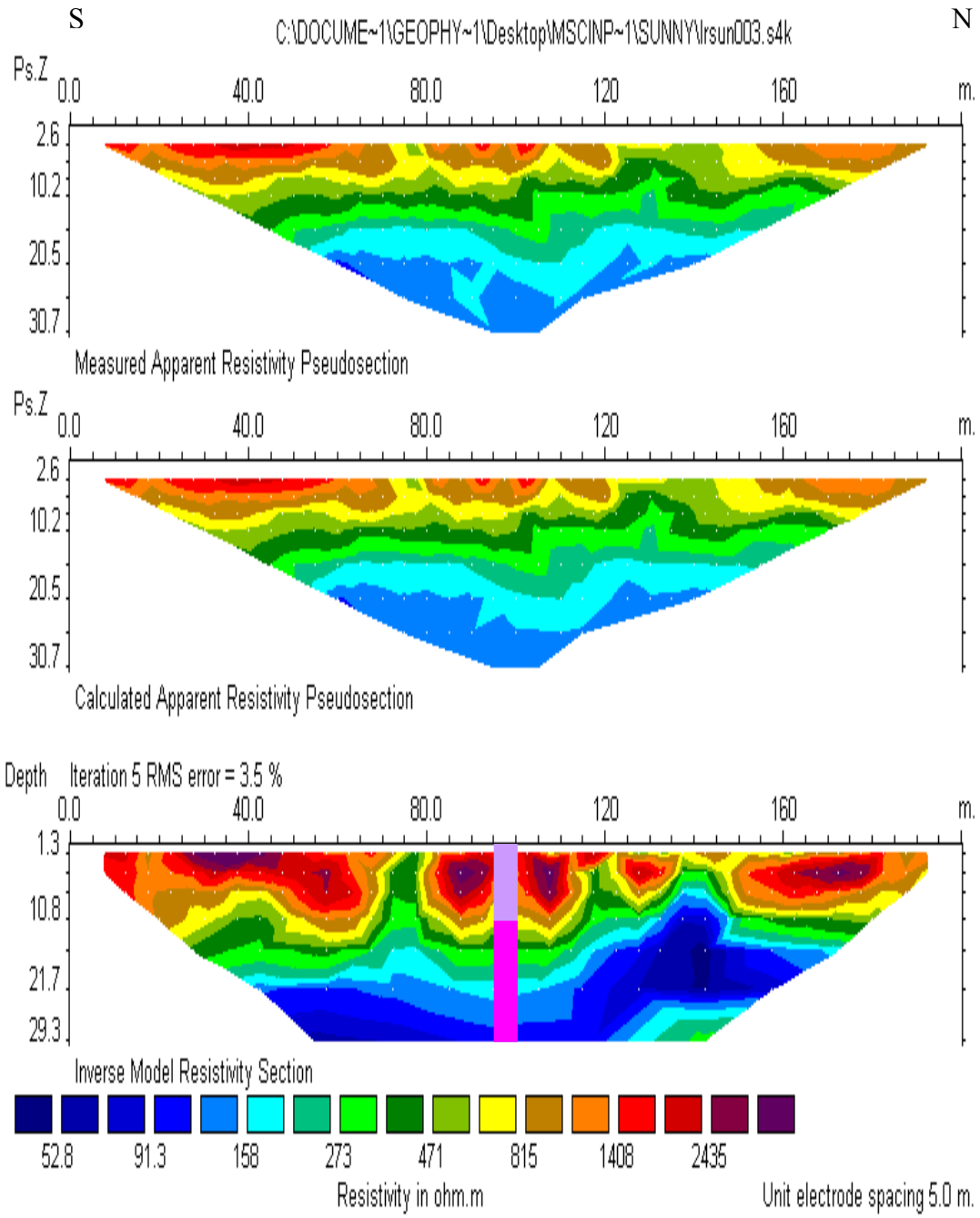


Figure 4.4 The result of 2D inversion of the Wenner-array data along survey line 3, in the ABUTH hostel.

Figure 4.5 shows resistivity inversion results (iteration 6, 5.4% total average RMS error), for profile 4. Thus indicating that good fits between the measured (observed) and calculated apparent resistivity data were achieved. A thin layer of resistivity anomaly (<148 Ωm - >542 Ωm) on the top indicates the presence of surface water in silt, sand and clay. Gravel and sand and consolidated laterite (<542 Ωm – >1036 Ωm) is also seen at the surface to a depth of over 16 m below the surface. Gravel and sand is sandwiched by consolidated laterite. The weathered basement continues from this depth to the fresh basement. The weathered basement shows variable resistivity (< 148 Ωm – 542 Ωm) signifying fractured crystalline rock which has weathered into clay, sand and gravel constituting the aquifer. Also a very low resistivity zone (<21.2 Ωm – >77.6 Ωm) is seen in this layer. This is a fracture zone in the bedrock believed to hold water. The increased thickness of weathering here provides a good reservoir with a higher probability of bedrock fracturing. The fresh crystalline basement is not revealed in this image, so it is likely at a depth greater than 30 m. Patches of unweathered bedrock (>1980 Ωm) is observed close to the surface below the 40 m and 80 m marks. This pseudosection correlated well with the borehole logs obtained from the Preussag Ltd and ABUTH hostels, as shown in figures 4.8 and 4.10 of section 4.5.

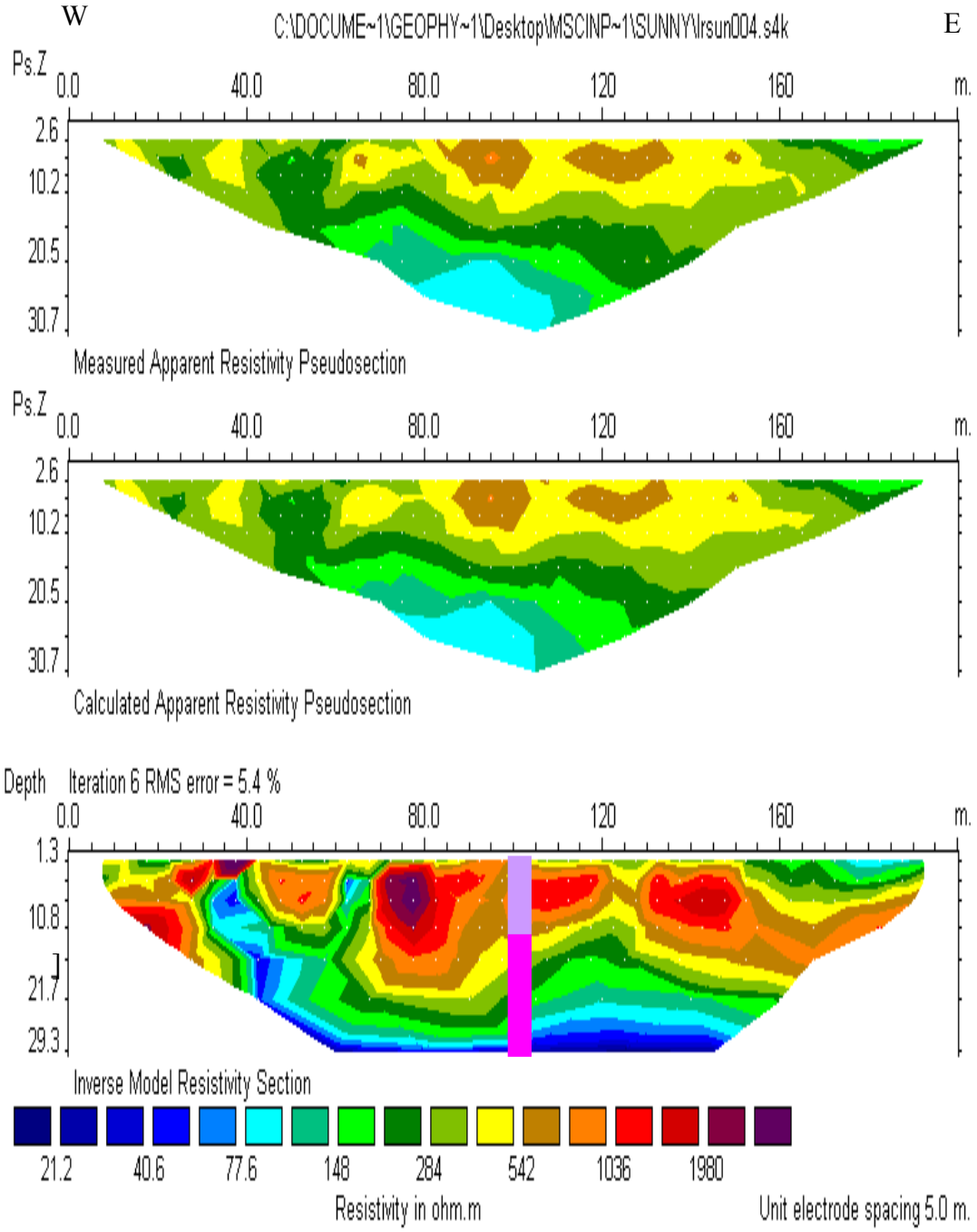


Figure 4.5 The result of 2D inversion of the Wenner-array data along

Survey line 4, in the ABUTH residential quarters.

Figure 4.6 shows resistivity inversion results (iteration 6, 3.6% total average RMS error), for profile 5. Thus indicating that good fits between the measured (observed) and calculated apparent resistivity data were achieved. A high resistivity anomaly (<78.1 Ωm - >755 Ωm) is seen in the top of the image and constitutes the overburden, having a thickness of about 15 m. This layer is made up of silt, clay, sand, and brownish consolidated laterite. There was probably a filling of laterite some time ago. A thick weathered basement (<78.1 Ωm - >355 Ωm) composed of gravel, sand and clay grades into the fresh basement at a depth greater than 30 m. This is the aquiferous layer. The increased thickness of weathering here provides a good reservoir with a higher probability of bedrock fracturing. Hence, there is a narrow vertical low resistivity zone (<8.08 Ωm – >36.7 Ωm) with a width of less than 10 m (but increases downwards) below the 85 m mark, which is probably a fracture zone in the bedrock trapping groundwater in the aquifer streaming to the surface. This position would be the best location to site a borehole in the area. The depth to the fresh crystalline basement is greater than 30 m. This pseudosection correlated well with the borehole logs obtained from the Preussag Ltd and ABUTH hostels, as shown in figures 4.8 and 4.10 of section 4.5.

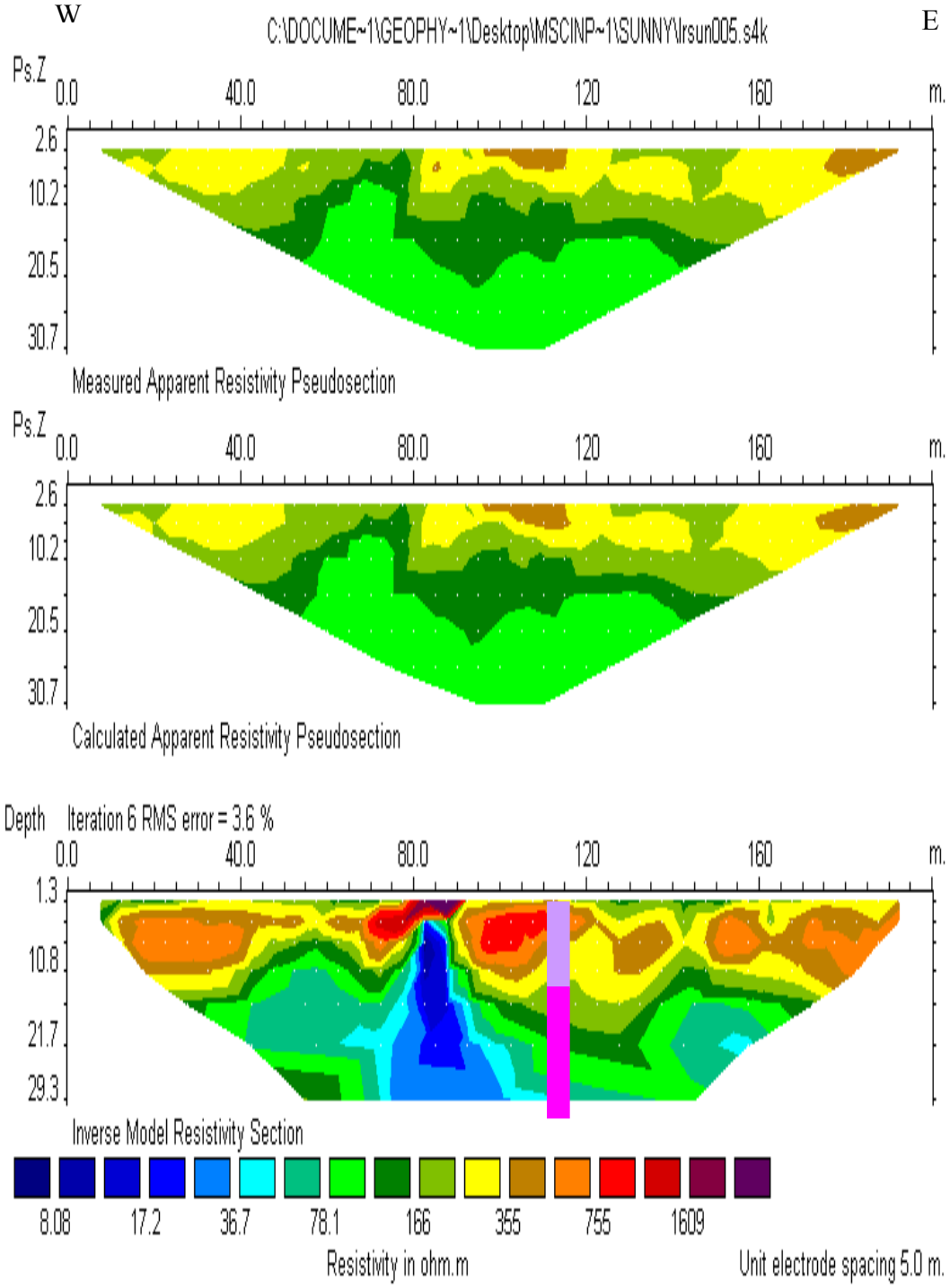

W
C:\DOCUME~1\GEOPHY~1\Desktop\MSCINP~1\SUNNY\Irsun005.s4k
E
Ps.Z
0.0
40.0
80.0
120
160
m.
2.6
10.2
20.5
30.7
Measured Apparent Resistivity Pseudosection
Ps.Z
0.0
40.0
80.0
120
160
m.
2.6
10.2
20.5
30.7
Calculated Apparent Resistivity Pseudosection
Depth
Iteration 6 RMS error = 3.6 %
0.0
40.0
80.0
120
160
m.
1.3
10.8
21.7
29.3
Inverse Model Resistivity Section
8.08
17.2
36.7
78.1
166
355
755
1609
Resistivity in ohm.m
Unit electrode spacing 5.0 m.

Figure 4.6 The result of 2D inversion of the Wenner-array data along survey line 5, in the ABUTH residential quarters

Figure 4.7 shows resistivity inversion results (iteration 7, 5.8% total average RMS error), for profile 6. Thus indicating that good fits between the measured (observed) and calculated apparent resistivity data were achieved. The image shows a large thickness of weathered rock covering the crystalline bedrock. The overburden is composed of gravel, sand, clay and silts (<260 Ωm - >1759 Ωm), consolidated laterite. Unweathered bedrock material (<1759 Ωm – >4578 Ωm), is also seen as part of a road traversed by the profile at the 105 m – 120 m marks. Other isolated patches of laterite traversed by the profile are seen at the 95 m, 140 m and 155 m marks. The weathered basement contains a low resistivity zone (<14.7 Ωm – > 99.7 Ωm) as seen rising to the surface at the 100m and 185m marks. This is probably a fracture zone containing water. This weathered basement grades into the fresh crystalline basement.

There is a prominent high resistivity anomaly >11918 Ωm, near the centre of the pseudosection. This is seen near the surface at the 110 m mark and this is possibly a cave or cavity. The inversion model gives the depth to the top of the cave at around 5 m. However, the degree of weathering is appreciably good and the increased thickness of weathering here provides a good reservoir that enhances bedrock fracturing. The depth to the fresh basement is greater than 30 m, so it is not revealed by the image. This pseudosection correlated well with the borehole logs obtained from Messrs Preussag Ltd and ABUTH hostels, as shown in figures 4.8 and 4.10 of section 4.5.

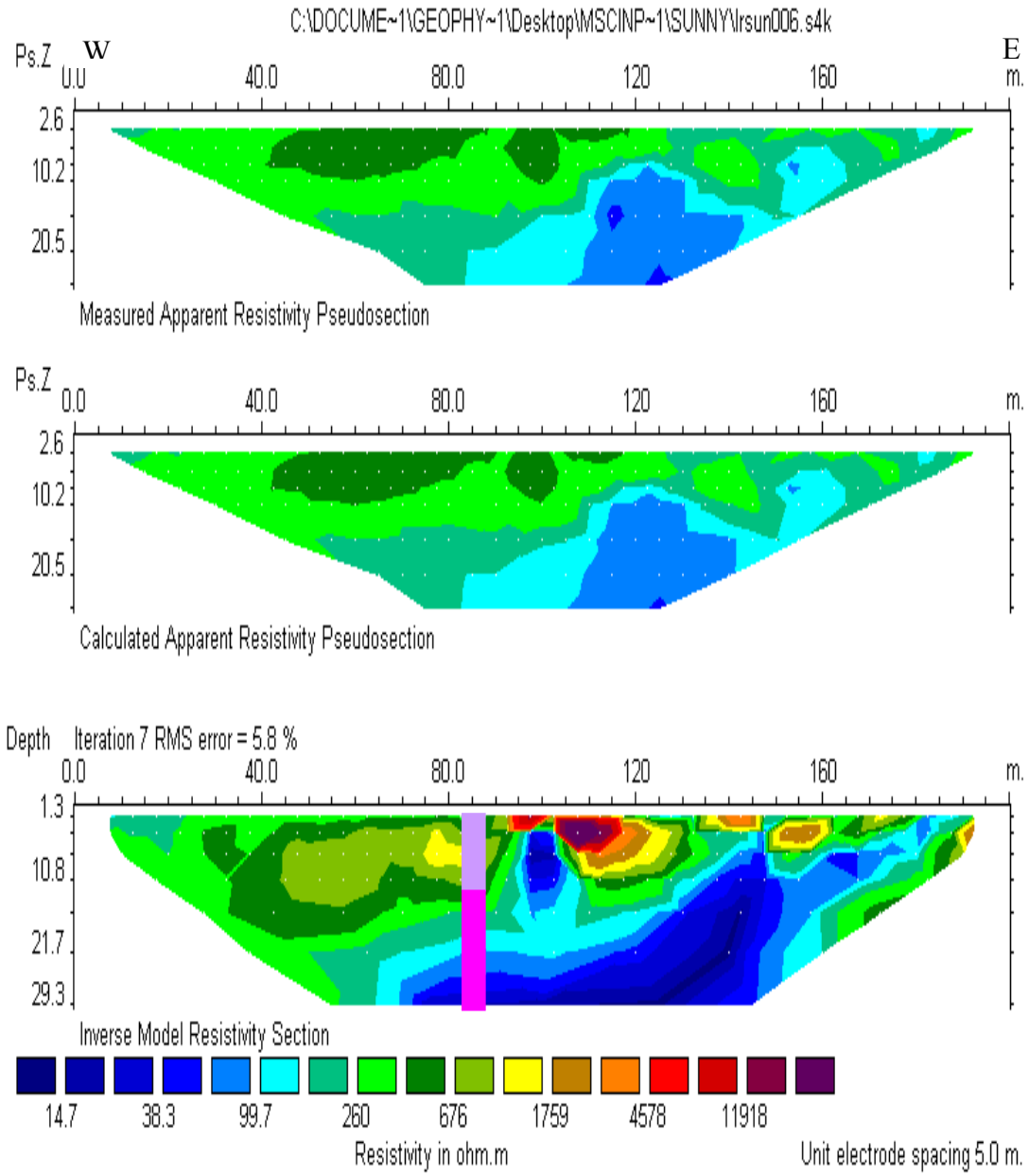


Figure 4.7 The result of 2D inversion of the Wenner-array data along survey line 6, in the ABUTH residential quarters.

For each profile, the sand and gravel, and consolidated laterite top layer corresponded to a high resistivity, the basement and patches of it found in the sections corresponded to the highest resistivity, and the weathered basement with clay corresponded to the intermediate and lowest resistivity values. The low resistivity of the weathered basement is due to its water content. However, resistivity ranges are usually determined by superimposing the boreholes over the electrical resistivity image and observing the correlation between the borehole lithology and the image resistivity.

However, correlation between the field results obtained shows that the overburden depth is the main factor controlling the electrical resistivity of the near- surface material. Overburden is generally, though not always, more conductive than the underlying bedrock. This is due to the high porosity and, hence, higher water content, and to a generally higher content of electrically conductive clay minerals relative to the bedrock. These results are in agreement with the results of the two-dimensional seismic refraction tomography survey carried out in the study area by my colleague.

4.5 Geologic Section from Borehole Data

Boreholes are a necessary and reliable source of primary data, and electrical resistivity imaging interpretations provide secondary information. Although borehole data provides a good sample for a six-inch diameter vertical cylindrical volume, it can be a poor representation of the several square metres surrounding the borehole. Alternatively, electrical resistivity imaging provides block averages of resistivity. Also, borehole data can be a more expensive data acquisition method when compared to an ERI survey.

The 2D inversion results of the survey were correlated with the lithology information obtained from the boreholes in Jama'a village, and the hostels and the residential quarters of ABUTH. The stratigraphic structure of the study area is very complex and is a product of volcanic and magmatic activities of various ages. A complete set of borehole logs used in this research can be found in the original hydrogeologic assessment report of the groundwater research department of the National Water Resources Institute (NWRI), Mando, Kaduna; Kaduna State, Nigeria. The geological well-log (Figure 4.8) determined by Messrs. Preussag Limited (Drilling Engineers), shows that the topsoil in the north-eastern part of the basin, around Jama'a Kubanni village, is lateritic consisting of clayey, silty and brownish material which may be up to 9m thick in the area (Olufemi, 1985). The layer below this is about the same thickness and consists of fine sand and partly silty and greyish material. These two layers overlay the weathered basement rock, which consists of fine to medium sand. The sand is clayey and contains quartz and feldspars and it is brownish in colour. The section shows that, at the depth of 36 m, fresh basement rock was encountered. The geologic section from the borehole log is shown in figure 4.8.

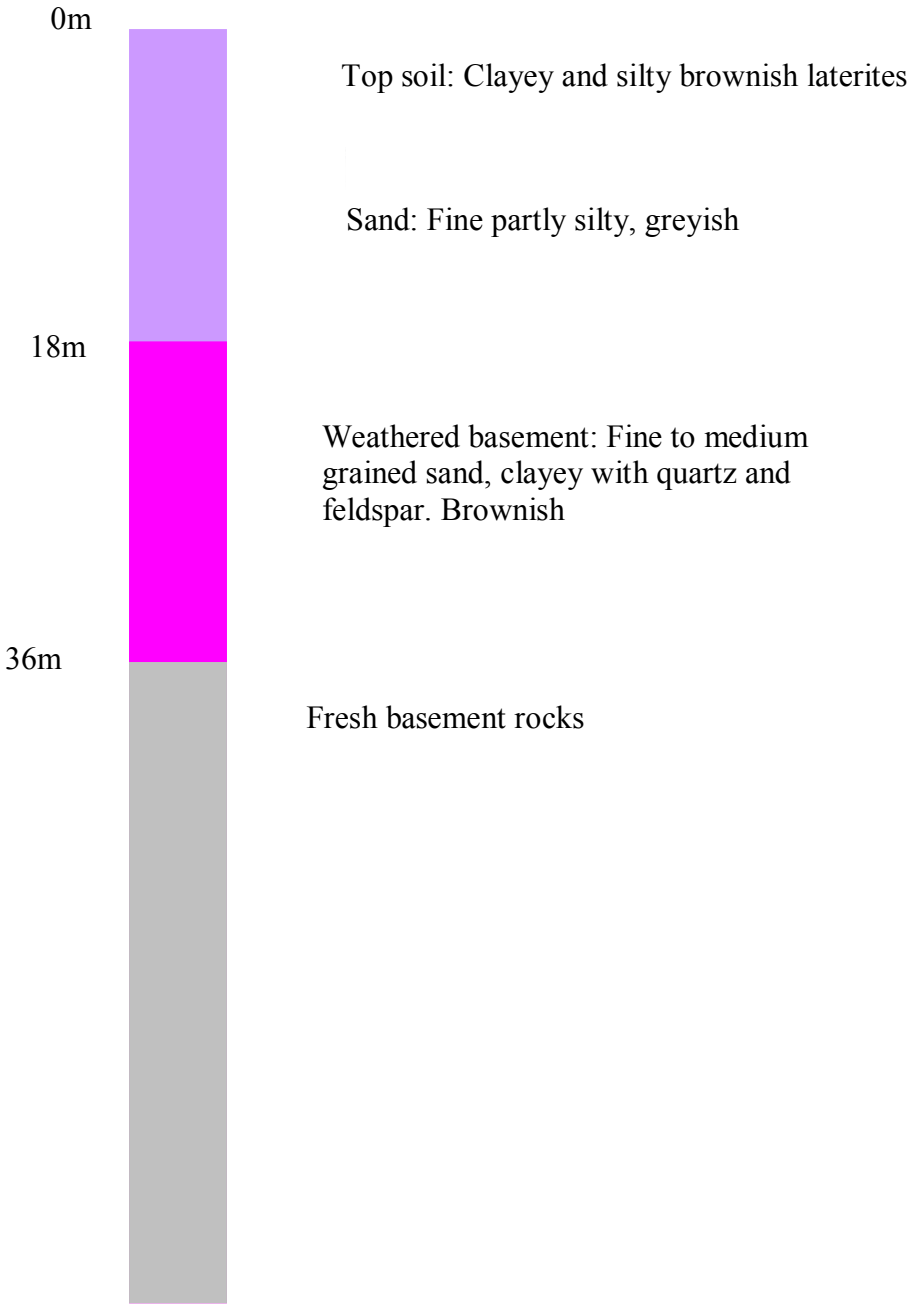


Figure 4.8 Geological Well-Log obtained by Preussag Ltd. (After Olufemi, 1985)

The second of these logs was that of a borehole in Shika town, (see figure 4.9), and shows an overburden made up of two layers 16 m thick. The first layer is composed of reddish brown lateritic clay top soil 9 m thick. The second layer is made up of a brownish sandy clay material about 7 m thick. The weathered basement lies immediately beneath the overburden and is about 5 m thick. The fresh crystalline basement rock is encountered at a depth of 21.3 m and is believed to extend continuously downward from this depth. The geologic section from the borehole is shown in figure 4.9.

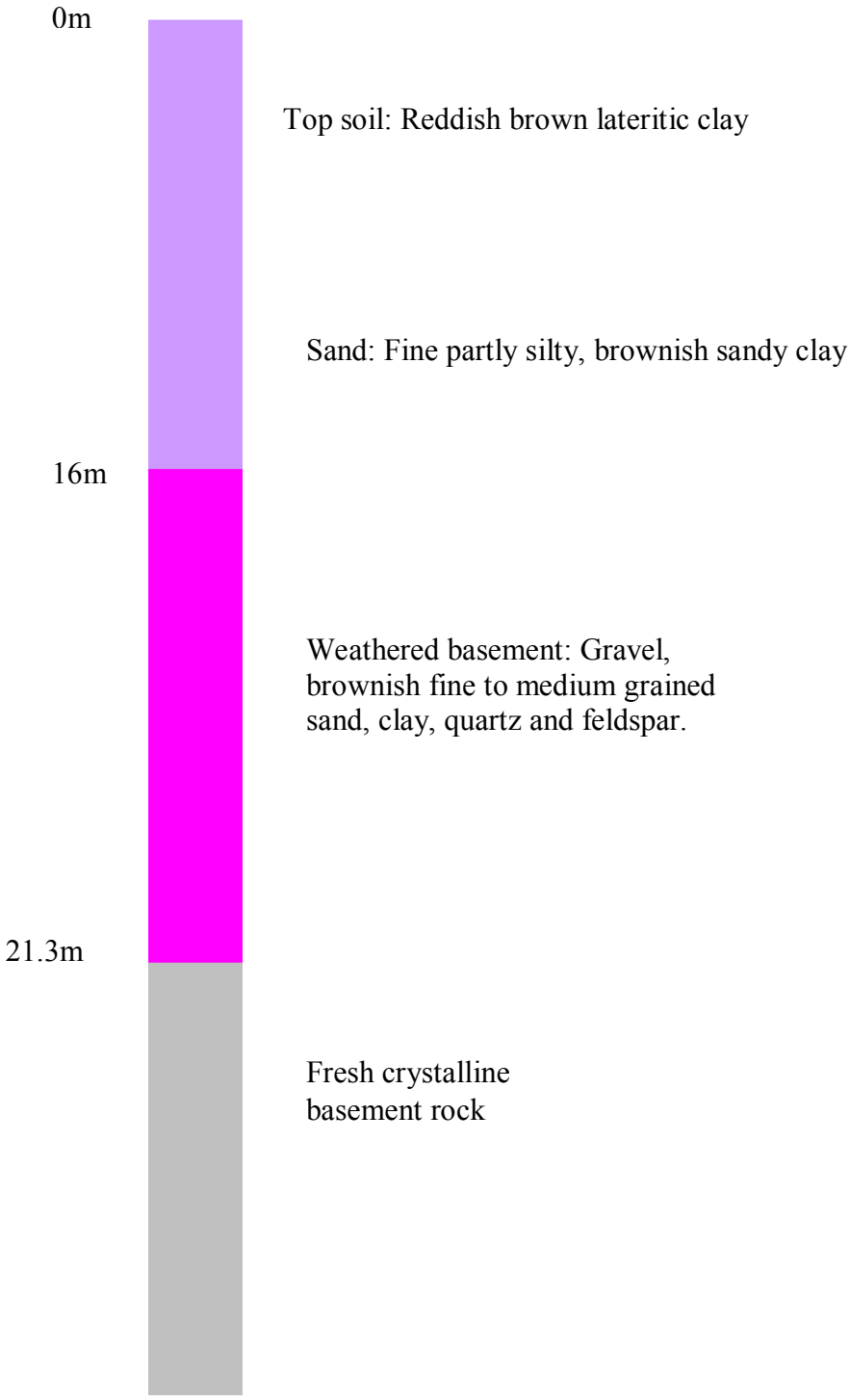

0m
Top soil: Reddish brown lateritic clay
Sand: Fine partly silty, brownish sandy clay
16m
Weathered basement: Gravel, brownish fine to medium grained sand, clay, quartz and feldspar.
21.3m
Fresh crystalline basement rock

Figure 4.9 Geological Well-Log of Shika obtained from the NWRI 2, Mando, Kaduna. (2002)

The third borehole log was that of a borehole in the hostels (figure 4.10), which reveals an overburden of about 26 m thickness, made up of brownish red lateritic soil, sand clay and clayey sand. This is the first layer. The weathered basement is composed of disintegrated schistose rock materials about 5 m thick and this second layer constitutes the aquifer. The fresh basement was encountered at a depth of 40 m. Both logs are similar, showing three distinct layers of similar constituents. The geologic section from the borehole is shown in figure 4.10.

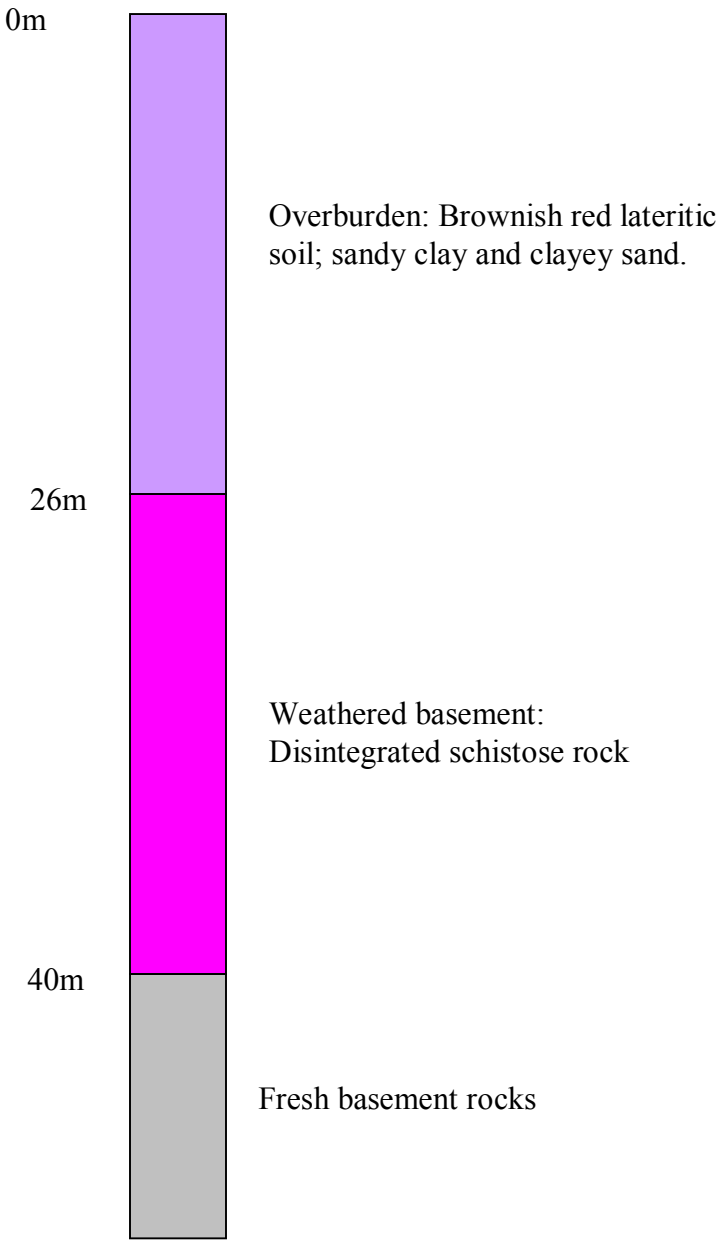


Figure 4.10 Geological Well-Log of ABUTH hostel obtained from the NWRI 1, Mando, Kaduna. (2002).

The lithology obtained from the boreholes provides a good representation of the stratigraphic sequence of the area. Resistivity values from the present research work and previous works were also used in the analysis.

4.6 Resistivity Values from the Research Work

Ranges of resistivity values obtained from the research work and from previous works in the environs of the study area are presented here, for comparison and analysis.

Table 4.1 Resistivity Values from the Research Work

Rock Type	Resistivity (Ωm)
Clay – fresh water	0.687 – 77.6
Dry – clay	52.8 – 158
Sand and gravel	99.7 – 190
Laterite	355 – 1759
Weathered basement	216 – 678
Fresh crystalline basement	1223 – 11,918

4.6.1 Typical Resistivity Values from Previous Works

Also resistivity values obtained from previous works within and close to the study area were used to correlate the results of the present survey, and these are considered in this section. Representative resistivity values of earth materials in the study area were derived from the works of Ososami (1968) and that of Messrs Preussag Ltd as contained in Olufemi (1985). These values were compared with the result of Baimba (1978) and Okwueze (1978) who also worked in different basement areas of Kaduna State. From these works and the resistivity values of various types of earth materials suggested by other authors, the representative resistivity values presented in Table 4.1 were compiled as a guide for the present work.

Based on the general representative resistivity values and the geological control (borehole logs) discussed above, the resistivity values shown in tables 4.1, 4.2a and 4.2b were used for the interpretation of the results of this work. However, the fact that these resistivity values were gotten from the use of earlier equipment like the Terrameter SAS 300C was considered.

Table 4.2a Typical Resistivity values compiled from previous works (Shemang (1990); Aminudeen (1990); Hassan, Ajayi and Ojo (1991) and Baimba (1978)).

Rock type	Resistivity (Ωm)
Clay – fresh water	30-70
Dry clay	40-100
Weathered basement	50-100
Laterite	200-400
Slightly weathered basement	200-500
Dry sand	500-1000
Fresh basement (crystalline)	>1000

Table 4.2b Typical Resistivity values compiled from previous works (Ameloko, A. A., 2006).

Rock type	Resistivity (Ωm)
Fadama loam	30-90
Clay, silt and sand (topsoil)	100-200
Sand and gravel	100-180

Weathered laterite	200-500
Fresh laterite	500-600
Weathered basement	20-100
Fresh basement	> 1000

The above results show that 2D surveying can form a powerful geological mapping tool, for use in engineering and environmental applications, including hydrogeological mapping. In combination with a limited number of drilling reference points, with locations based on the resistivity results, reliable models of the subsurface can be created. In cases where as much detailed information as possible on the layer sequence is required, VES analysis of selected data is a useful tool. However, this only applies where the lateral variation is small, which can be accessed from the pseudosection and depth sections.

CHAPTER FIVE

DICUSSION OF RESULTS, SUGGESTIONS AND CONCLUSIONS

5.1 Discussion of Results

The models obtained from 2D inversion of the field data using different starting models mainly showed that the inversion algorithm is stable. After that, comparison of the measured apparent resistivity pseudosection and the calculated apparent resistivity pseudosection resulted in a reasonably good agreement with the inverse model resistivity section. As a result, this demonstrates the stability of the 2D inversion algorithm that can give reliable models. Based on the electrical images obtained in the study area, three distinct layers were revealed.

(i) **The Overburden**: this is made up of two parts, the topmost of which is about 9 m thick and is composed of reddish brown lateritic clay. The second part is about 7 m thick and is composed of brownish sandy clay. Combining these two parts together reveals an overburden with an average thickness of about 16 m – 26 m which agrees with the borehole logs.

(ii) **The Weathered Basement**: the overburden is immediately underlain by the weathered basement which consists of disintegrated schistose rock materials, sand and gravel. This layer has a relatively low resistivity due to the presence of water and clay, which reduces the permeability, so this layer is thus regarded as the aquifer as it usually holds water. Also, the layer is highly weathered and the degree of weathering increases toward the southern part of the study area. This increased thickness of bedrock weathering is a proof of the capability of this layer to provide a good reservoir with a

higher probability of the presence of fractures in the basement. The average thickness of this layer is about 5 m – 14 m. Thus, this correlates well with the borehole logs of the site being investigated.

(iii) **The Fresh Bedrock**: the fresh basement rock was encountered at a variable depth of between 21 m and >30 m, in figure 4.3 and the rest of figures 4.4 to 4.7 respectively. The average depth of the fresh basement is about 40 m as provided by the borehole log (NWRI 1). The value of the resistivity of the basement rocks is appreciably high, rising from 1223 Ωm up to 11918 Ωm which is indicative of typical crystalline bedrock. This layer is believed to grade indefinitely or infinitely downward. The average depth of penetration is about 29.3 m. The basement though fresh, is frequently fractured which gives it a high permeability. But as fractures do not constitute a significant volume of the rock, fractured basement has low porosity.

5.2 Groundwater Potentials

Groundwater modelling is a rapidly evolving field in hydrology. Groundwater systems can be simulated, allowing predictions to be made about the effects of aquifer exploitation on water quantity and water quality. The reliability of the results of such numerical model studies largely depends upon the amount of available parameter data that are fed into the model, and their precision. Geophysical exploration methods can provide parameter data, such as the geometry of aquifers and of less permeable layers and the salinity of the groundwater. The electrical images indicate large thicknesses of weathered materials overlaying the basement rocks. Also fractures are not visibly indicated and the increased thickness of weathering provides a good reservoir with a

higher probability of bedrock fracturing (Acworth, 1987). These form the aquifer in the study area. To site successful boreholes to tap groundwater in hard rock or basement terrains is a complex problem because of the heterogeneous nature of the aquifer system. But as fractures do not constitute a significant volume of the rock, fractured basement has low porosity.

For this reason a good borehole providing long term high yields is one which penetrates a large thickness of regolith, which acts as a reservoir and also intersects fractures in the underlying bedrock, the fractures providing the rapid transport mechanism from the reservoir and so hence the high yield. Boreholes which intersect fractures, but which are not overlain by thick saturated regolith, cannot be expected to provide high yield in the expected long term. A borehole which penetrate saturated regolith but which find no fractures in the bedrock is likely to provide sufficient yield for a hand pump only. However, only electrical methods can provide data on water quality, which is one of the reasons why they have become so successful in groundwater exploration. Considering the established geoelectric parameters as well as topographic, geologic and hydrogeological implications, groundwater potential of the site could be considered as reasonably encouraging for borehole development.

5.3 Suggestions for Future Work

The electrical imaging technique is not a reconnaissance tool. It is suitable for the detailed study of problem areas that have been selected using other techniques, such as Electromagnetic Method (EM) or resistivity traversing.

Finally, future work should be extended beyond the limits of the profiles traversed in this work for better understanding of the subsurface, and also the roll-along CVES

surveying method of probing the subsurface should be employed to give a better coverage at depth. 3D resistivity survey should be undertaken in the survey area.

5.4 Conclusions

By comparing RES2DINV resistivities with the results of resistivities from past works and those of standard texts, it was found to correlate quite well in the various layers. Also by comparing RES2DINV resistivity values with the results of available borehole logs of the boreholes in the survey area and its environs, it was found that the resistivity values correlates quite well with the geological formations revealed by the borehole logs. This then lend credence to the fact that the electrical imaging method has in the past proved to be a powerful technique in the study of subsurface geology. This is because electrical images provide a detailed view of subsurface structure than can be obtained using any other geophysical techniques and may therefore, lead to a better understanding of the local geology and hydrogeology.

Three layers were seen as reflected on the sections presented in this work. These layers are made up of a brownish red lateritic/silty clay top layer, the schistose, gravely sand transition zone of the basement rock which is the aquifer and the fresh basement.

The depth to the basement is variable, being shallower in the northern part of the study area and deeper towards the southern part. This result agrees with previous works in the area (Hassan, 1991) and (Ososami, 1986). They observed that the bedrock generally gets deeper towards the southern part of the study area. In profile 2 the basement is prominently reflected at an average depth >21.7 m and dips toward the south

while the other profiles reveal the presence of the basement rock at depths well beyond 30 m. These results agree with the results of the seismic refraction tomography survey conducted in the study area by my partner.

Although 3D resistivity techniques are being developed rapidly, 2D surveying will probably in many applications remain the most useful for logistic and cost reasons. A number of 2D profiles can be combined to compile quasi 3D models.

REFERENCES

ABEM Instrument AB, Terrameter SAS4000 LUND Imaging System, Instruction Manual.

Acworth, R. I., 1987. The development of crystalline basement aquifers in a tropical environment. *Quarterly Journal of Engineering Geology*. **Vol**. 20. Pp. 265-272.

Adamu, A. G., 1973. Basement geology of Zaria-Samaru Area, An Unpublished B.Sc. project, Department of Geology, Ahmadu Bello University, Zaria.

Akpoborie, I. A. 1972. Hydrogeological Control of Structures along Samaru Creek. Unpublished B. Sc. Thesis. Department of Geology. Ahmadu Bello University, Zaria.

Ameloko A.A. 2006. Two-dimensional Imaging over the western part of the Kubanni River Basin, Zaria, Nigeria. An unpublished M.Sc. Thesis. Department of Physics.Ahmadu Bello University, Zaria.

Aminudeen, A. I. 1990. Geoelectrical investigations for groundwater in four villages in Roni Local Government Area, Kano State, Nigeria. Unpublished M.Sc. Thesis, Department of Physics, Ahmadu Bello University, Zaria.

Baimba, A.B. 1978. Resistivity and refraction seismic methods for groundwater exploration at Zango, Kaduna state. Unpublished M. Sc. Thesis. Department of Physics. Ahmadu Bello University, Zaria.

Barker R.D. 2001. Imaging fractures in hardrock terrain. Research Note 2. University of Birmingham, UK. Pp. 1 – 4.

Barker R., Venkateswararao T. and Thangarajan M. 2001. Electrical imaging for borehole siting in India. Research Note 3. University of Birmingham, UK. Pp. 1 – 7.

Batayneh, A. T. 2006. Resistivity tomography as an aid to planning gas-pipeline construction, Risha area, north-east Jordan. *Near Surface Geophysics*, **Vol**. 4, Pp. 313 – 319.

Cardarelli, E. and Fischanger, F. 2006. 2D data modelling by electrical resistivity tomography for complex subsurface geology. *Geophysical Prospecting*, **Vol**. 54. Pp. 121 – 133.

Dahlin T. 1996. 2D resistivity surveying for environmental and engineering applications. *FIRST BREAK*. **Vol**. 14 (7). Pp. 275 – 283.

Dobrin, M. and Savit, C.H. 1988. *Introduction to geophysical prospecting*. McGraw Hill Book Company. New York.

Dobrin, M. 1976. *Introduction to geophysical prospecting*. McGraw Hill Book Company. New York.

Eigbefo, C. 1978. Hydrogeology of the Kubanni Drainage basin, Zaria. Unpublished M. Sc. Thesis. Department of Geology, Ahmadu Bello University, Zaria.

Grant, F.S. and West, G.F. 1965. *Interpretation theory in applied geophysics*. McGraw Hill Book Company. New York.

Grant, N. K. 1969. The late Precambrian to early Paleozoic pan African Orogeny in

Ghana, Togo, Dohomey, and Nigeria. Geol. Soc. Am. Bull., **Vol**. 80. Pp. 45-56.

Griffiths, D. H. and Barker, R. D. 1993. Two-dimensional resistivity imaging and modeling in areas of complex geology. Journal of Applied Geophysics. **Vol**. 29. Pp. 211 – 226.

Griffiths, D. H., Turnbull, J. and Olayinka, A. I. 1990. Two-dimensional resistivity mapping with a computer-controlled array. First Break **Vol**. 8 (4), Pp. 121 – 129.

Hassan, M., Ajayi, C. O. and Ojo, S. B. 1991. A Basement structure determined from Geoelectric mapping of the Kubanni River Basin, Zaria: Nigerian Journal of Physics, **Vol**. 3. Pp. 166-173

Joda, F.O. 1990. The establishment of a local gravity network for Zaria area. Unpublished M.Sc. thesis. Department of Physics, Ahmadu Bello University, Zaria.

Keary,P. and Brooks, M., 1988. An Introduction to Geophysical Exploration. Blackwell Scientific Publication. London.

Koefoed, O. 1979. Geosounding Principles, 1: Resistivity Sounding measurements. Elsevier press.

Loke, M.H. and Barker, R.O. 1996. Rapid least-squares inversion of apparent resistivity pseudosections by a quasi-Newton method. *Geophysical prospecting*. **Vol**.44: Pp. 135-152.

McCury, P. 1970. The geology of Degree Sheet 21, Zaria. Unpublished M.Sc. thesis. Department of Geology, Ahmadu Bello University, Zaria.

McCury, P. 1976. The geology of the Precambrian to Lower Paleozoic rocks of Northwestern Nigeria. A review in Kogbe, C.A. (Ed), *Geology of Nigeria*. Elizabethan Publishing Company, Lagos. Pp. 15-39.

Meads, L.N., Bently, L. R. and Mendoza, C. A.. 2003. Application of electrical resistivity imaging to the development of a geologic model for a proposed Edmonton landfill site. *Canadian Geotechnical Journal*. **Vol**. 40. Pp. 551-558.

National Water Resources Institute (NWRI, 1). 2002. Groundwater Research Development. Completion Report. Borehole NR. GWR/HG-05(1/6), January 2002.

National Water Resources Institute (NWRI, 2). 2002. Groundwater Research Development. Completion Report. Borehole NR. HGD/IAR/01(1/6), May 2002.

Okwueze, E. E. 1978. Geophysical exploration for groundwater in Kankarg Kaduna State. Unpublished M. Sc. Thesis. Department of Physics, Ahmadu Bello University, Zaria.

Olayinka, A. I. and Barker, R. D. 1990. Borehole siting in crystalline basement areas of Nigeria with a microprocessor-controlled Resistivity Traversing System. *Ground Water*. **Vol**. 28. Pp. 178 – 183.

Oldenburg, D.W. and Li, Y. 1999. Estimating depth of investigation in D.C. Resistivity and IP surveys. *Geophysics*. **Vol**. 64 (2). Pp. 403-416.

Olowu, D., 1967. Preliminary investigation of the groundwater conditions in Zaria, sheet 102 SW: *GSN report* No. 1462.

Olufemi, R. O., 1985. Hydrogeology of Jama'a Kubanni Area. (Zaria Sheet 102 SW). Unpublished B. Sc. Thesis. Department of Geology, Ahmadu Bello University, Zaria

Oluyide, P. O. and Udoh, A. 1986. Major fracture system of Nigeria. In press.

Ososami, I. A. 1968. Assessment of the groundwater in the Kubanni Valley. Unpublished M. Sc. Thesis. Ahmadu Bello University, Zaria.

Oyawoye M. O. 1964. Geology of the Nigerian Basement Complex, Journal of Nigeria Mining, Geological and Metallurgical Society Vol. Pp. 87-102.

Özürlan, G., Candansayar, M.E. and Şahin M. H. 2006. Deep resistivity structure of the Dikili-Bergama region, west Anatolia, revealed by two-dimensional inversion of vertical electrical sounding data. *Geophysical Prospecting*. **Vol**. 54. Pp. 187 – 197.

Raji, B.A. 1986. Evaluation of groundwater for irrigation in the Asa (Kwara State) and Shika (Kaduna State) drainage basins. Unpublished M.Sc. thesis. Department of Geology, Ahmadu Bello University, Zaria.

RES2DINV ver.3.4 Geoelectrical Imaging 2D and 3D *GEOTOMO SOFTWARE* August 2001.

Russ, W. 1957. The geology of part of Niger, Zaria and Sokoto provinces with special reference to the occurrence of gold. Bulletin: *Geological survey*, Nigeria. **No**. 27. Pp. 42.

Shemang E. M. 1990. Electrical depth soundings at selected well sites within the Kubanni River Basin, Zaria, Unpublished M. Sc Thesis. Department of Physics, Ahmadu Bello University, Zaria.

Sheriff, R.E. 1976. *A first course in exploration and interpretation*. International Human Resources Development Corporation. Boston.

Telford, W. M. Geldart, L. P. Sherif, R. E. and Keys, D. A., 1990. Applied Geophysics. Cambridge University Press. New York.

Tokarski, A. 1972. Heterogeneous Terrace Arrangement West of Ahmadu Bello University. occasional paper, No. 1, Department of Geology, Ahmadu Bello University, Zaria.

Trustwell, J.F. and Cope, R.W. 1963. The geology of parts of Niger and Zaria provinces, northern Nigeria. *GSN, Bulletin* 29.

Umar, F.A. 2001. Geoelectric investigation of the groundwater potential in the Institute of Agricultural Research (IAR) farm, Samaru, Zaria. Unpublished M.Sc. thesis. Department of Physics, Ahmadu Bello University, Zaria.

Wright, J.B. and McCury, P. 1970. The geology of Nigeria Sheet 102 SW, Zaria and its regions. Edited by M.J. Mooretimore. Department of Geography, Occasional Paper, **No**. 4, Ahmadu Bello University, Zaria.